Title
Panoply of P: An Array of Rhenium—Phosphorus Complexes Generated from a Transition Metal Anion

Journal
Inorganic Chemistry, 63(24)

ISSN
0020-1669

Authors
Hales, David P
Rajeshkumar, Thayalan
Shiau, Angela A
et al.

Publication Date
2024-06-17

DOI
10.1021/acs.inorgchem.4c01085

Panoply of P: An Array of Rhenium-Phosphorus Complexes Generated from a Transition Metal Anion

David P. Hales,† Thayalan Rajeshkumar,§ Angela A. Shiau,‡ Guodong Rao,‡ Erik T. Ouellette,† Robert G. Bergman,† R. David Britt,‡ Laurent Maron,§ John Arnold†*

†Department of Chemistry, University of California, Berkeley, California 94720, United States

‡Department of Chemistry, University of California, Davis, California 95616, United States

§LPCNO, Université de Toulouse, INSA Toulouse, 135 Avenue de Rangueil, Toulouse 31077, France

ABSTRACT: We expand upon the synthetic utility of anionic rhenium complex Na[(BDI)ReCp] (**1**, BDI = N,N′-bis(2,6-diisopropylphenyl)-3,5-dimethyl-*β*-diketiminate) to generate several rhenium-phosphorus complexes. Complex **1** reacts in a metathetical manner with chlorophosphines Ph_2PCl, ^{Me}NHP-Cl, and OHP-Cl to generate XL-type phosphido complexes **2**, **3**, and **4**, respectively (^{Me}NHP-Cl = 2-chloro-1,3-dimethyl-1,3,2-diazaphospholidine; OHP-Cl = 2-chloro-1,3,2-dioxaphospholane). Crystallographic and computational investigations of phosphido triad **2**, **3**, and **4** reveal that increasing the electronegativity of the phosphorus substituent (C<N<O) results in a shortening and strengthening of the rhenium-phosphorus bond. Complex **1** reacts with iminophosphane Mes*NPCl (Mes* = 2,4,6-tri-*tert*-butylphenyl) to generate linear iminophosphanyl complex **5**. In the presence of a suitable halide abstraction reagent, **1** reacts with the dichlorophosphine $^{i}Pr_2NPCl_2$ to afford cationic phosphinidene complex $\mathbf{6}^{+}$. Complex $\mathbf{6}^{+}$ may be reduced by one electron to form $\mathbf{6}^{\bullet}$, a rare example of a stable, paramagnetic phosphinidene complex. Spectroscopic and structural investigations, as well as computational analyses, are employed to elucidate the influence of the phosphorus substituent on the nature of the rhenium-phosphorus bond in **2** through **6**. Furthermore, we examine several common analogies employed to understand metal phosphido, phosphinidene, and iminophosphanyl complexes.

TOC Graphic

(see end of file)

INTRODUCTION

Complexes with metal-phosphorus (M–P) bonds are a cornerstone of organometallic chemistry, in large part due to the ability of phosphorus to form strong, covalent *σ*-bonds with most metals. The ubiquitous phosphine (PR_3) serves as a class of ligands for many of the most historically important and industrially relevant organometallic complexes.[1–4] In addition to forming strong, covalent M–P *σ*-bonds, phosphines are also sterically and electronically tunable, making them ideal spectator ligands for organometallic catalysts.[5–8] Metal phosphido ($M–PR_2$) and phosphinidene (M=PR) complexes are also synthetically useful species, albeit for different reasons than $M–PR_3$ complexes. While reactivity in $M–PR_3$ complexes typically takes place at the metal center, reactivity in $M–PR_n$ (n = 1, 2) complexes often directly involves the phosphorus center(s).[9–11] This makes the substituent at phosphorus, R, an even more important factor for modulating reactivity in $M–PR_n$ complexes. In general, electronegative R render a $M–PR_n$ complex *electrophilic* at phosphorus, while electropositive R render the $M–PR_n$ complex *nucleophilic* at phosphorus.[12–14]

Based on the phosphorus R substituent(s), as well as the identity of the metal and its ligand set, $M–PR_n$ complexes are often conceptualized as lying on the continuum between two ionic extremes. On one side of the extreme, a $M–PR_n$ complex can be considered to arise from the combination of a negatively charged $\{PR_n\}$ fragment (i.e. R_2P^- or RP^{2-}) with a high valent {M} fragment. On the other (less common) side of the extreme, a $M–PR_n$ complex can be considered to arise from the combination of a neutral or even positively charged $\{PR_n\}$ fragment (i.e. R_2P^+ or RP^0) with a low valent {M} fragment. These ionic extremes are a useful paradigm that assists with electron counting and quickly (albeit crudely) conveys the electronic structure of the M–P bond. It should be noted that the fundamental bonding interactions between the {M} and $\{PR_n\}$ fragments are independent of which depiction is ultimately chosen. The depiction chosen for a given $M–PR_n$ complex also need not mirror the method by which the complex is synthesized. To maintain consistency with the literature and minimize confusion we will default to the anionic formalism and nomenclature for $M–PR_2$, M–PNR, and M=PR complexes, but will strive to point out where this conception may be inadequate.

Surprisingly, there are very few examples of metal fragments for which several $M–PR_n$ complexes have been characterized, such that the influence of the R substituent might be systematically unraveled. One of the few frag-

ments for which several M–PR_n complexes have been synthesized is the classic iron system, $(CO)_2FeCp^\dagger$ (Figure 1, $Cp^\dagger$= Cp or Cp*; Cp* = 1,2,3,4,5-pentamethylcyclopentadienyl). Iron-phosphorus complexes of the type $(CO)_2Fe(PR_n)Cp^\dagger$ are primarily accessed via salt metathesis with the iron metalate $Na[(CO)_2FeCp^\dagger]$, and include iron-phosphido (Fe–PR_2),[15–28] phosphinidene (Fe=PR),[29,30] iminophosphanyl (Fe–PNR),[31] diphosphenyl (Fe–PPR),[32,33] and phosphaalkenyl (Fe–PCR_2)[17,34–37] complexes. The Fe–P bonds in these complexes have minimal π-character, a consequence of the filled a'' orbital in the d^6 $[(CO)_2FeCp^\dagger]^+$ fragment (Figure 1).[38] Correspondingly,

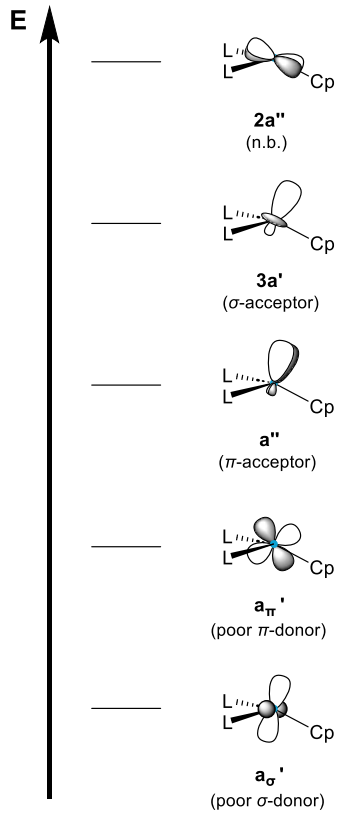

Figure 1. Qualitative frontier molecular orbital diagrams of the L_2MCp fragment.

$(CO)_2Fe(PR_n)Cp^\dagger$ type complexes are characterized by Fe–P single bonds and bent Fe–PR_n geometries. The analogous d^4 molybdenum fragment $[(CO)_2MoCp^\dagger]^+$, however, has an empty a'' orbital, which profoundly affects the nature of the Mo–P bond in $(CO)_2Mo(PR_n)Cp^\dagger$ type complexes. In contrast with the iron case, these complexes feature short Mo–P double bonds and planar/linear Mo–PR_n geometries. To our surprise, while several Mo–PR_2[39–54] and Mo–PCR_2[37,55,56] complexes of this type have been reported no Mo–PNR or Mo=PR complexes are yet known for the $[(CO)_2MoCp^\dagger]^+$ fragment. On the whole, $L_2M(PR_n)Cp^\dagger$ type complexes with a d^0, d^2, or d^4 configuration are rare.[57,58] We hypothesized that a bulky L_2MCp fragment with a low d^n configuration could serve as an excellent platform for the formation, stabilization, and comparison of M–PR_n complexes with strong M–P multiple bonding.

We recently reported the synthesis and reactivity of a rhenium metalate (**1**, Na[(BDI)ReCp]) capable of stabilizing many unusual bonding motifs.[59–68] The most common mode of reactivity for metalate **1** is salt metathesis, whereby **1** acts a source of the $[(BDI)ReCp]^+$ fragment. Like $[(CO)_2MoCp^\dagger]^+$, $[(BDI)ReCp]^+$ is a d^4 L_2MCp-type fragment, capable of forming strong π-interactions with ligand fragments of appropriate orbital symmetry. Unlike the molybdenum fragment, however, this rhenium fragment possesses a β-diketiminate ligand with considerable steric bulk, which serves to protect its complexes from deleterious reactivity. For these reasons, we anticipated that the (BDI)ReCp platform would serve as an excellent framework for the comparison of multiply-bonded M–PR_n (n = 1,2) complexes (Figure 2).

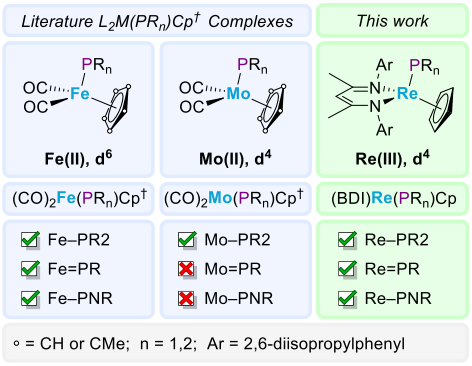

Figure 2. Comparison of $L_2M(PR_n)Cp^\dagger$ type complexes.

RESULTS AND DISCUSSION

Synthesis and Characterization of Rhenium Phosphido Complexes. We treated metalate **1** with several chlorophosphines in an equimolar ratio with the intention of forming Re–P bonds via salt metathesis reactions. Low temperature combinations of **1** with phosphorus trichloride (PCl_3) or dichlorophosphines ($PRCl_2$) unfortunately led only to the isolation of the previously reported complexes (BDI)ReCp and (BDI)Re(Cl)Cp.[59,66] We turned to monochlorophosphines (PR_2Cl) to increase the likelihood of a straightforward metathesis reaction. The reaction of **1** with chlorophosphines PPh_2Cl, ^{Me}NHP-Cl, and OHP-Cl were more productive, giving high yields of terminal phosphido complexes **2**, **3**, and **4**, respectively (Scheme 1).

In the NMR spectra for **2**-**4**, the ^1H signals for the ancillary ligands fall in the expected ranges for diamagnetic complexes and the ^{31}P signals fall in the expected range for planar phosphido complexes (Figures S1-S9).[69] In ^1H NMR spectra of **4** the OHP methylene protons are equivalent, indicating rapid interconversion of these protons at room temperature, presumably via rotation around the Re–P

Scheme 1. Synthesis of Phosphido Complexes 2, 3, and 4.

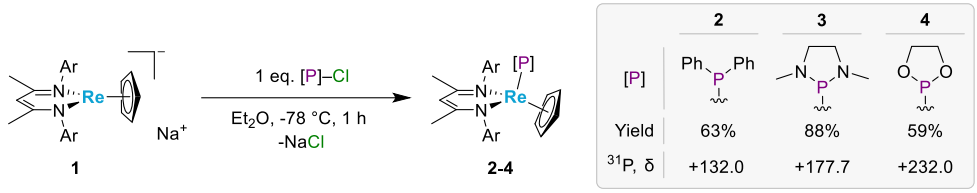

bond. The ^{Me}NHP methylene protons in complex **3**, on the other hand, are inequivalent in room temperature ^{1}H NMR spectra. Space-filling models of complex **3** reveal that steric repulsion between the BDI isopropyl groups and the ^{Me}NHP methyl groups likely restricts rotation around the Re–P bond in **3** (Figure S27). In complex **2** the overlap in ^{1}H signals of the phosphido phenyl groups and BDI aryl groups makes it difficult to draw such conclusions from NMR, but the space-filling model suggests that rotation around the Re–P bond in **2** is sterically prohibited. The trend in the chemical shift of ^{31}P signals in **2**-**4** (+132.0, +177.7, and +232.0 ppm, respectively) is consistent with the deshielding of the phosphorus nucleus by increasingly electronegative phosphorus substituents.[70] The ^{31}P resonance of **3** is considerably upfield of the ^{31}P resonance in $(CO)_2Mo(^{Me}NHP)Cp$ (+271 ppm), even though both are d^4 L_2MCp type systems.[71] This may be justified by comparing the relative basicities of the L_2 set in these complexes. While the BDI ligand in **3** is highly donating, the carbonyl ligands in the molybdenum case are strongly π-acidic. Correspondingly, the molybdenum center is less electron rich and the M–P bond is more polarized towards the metal in the molybdenum complex, deshielding the phosphorus nucleus.

Complexes **2**-**4** were analyzed by single crystal X-ray diffraction (XRD) to confirm structural assignments and determine relevant bond metrics (Figure 3). In phosphido complexes **2**, **3**, and **4**, the Re–P distances are 2.2125(5), 2.1607(8), and 2.144(2) Å and the sums of angles around phosphorus ($\Sigma\measuredangle^P$) are 358.08(13), 358.61(16), and 355.8(6)°, respectively (Table 1). The short Re–P bond

Table 1. Crystallographically Determined Bond Lengths for 2-4 (above) and Pyykkö Covalent Radii (below).

Complex or B.O.	Re–P (Å)	P–C (Å)	P–N (Å)	P–O (Å)
2	2.2125(5)	1.831(2) 1.836(2)	–	–
3	2.1607(8)	–	1.684(2) 1.697(2)	–
4	2.144(2)	–	–	1.637(9) 1.638(7)
Single	2.42	1.84	1.82	1.74
Double	2.21	1.69	1.62	1.59
Triple	2.04	1.54	1.48	1.47

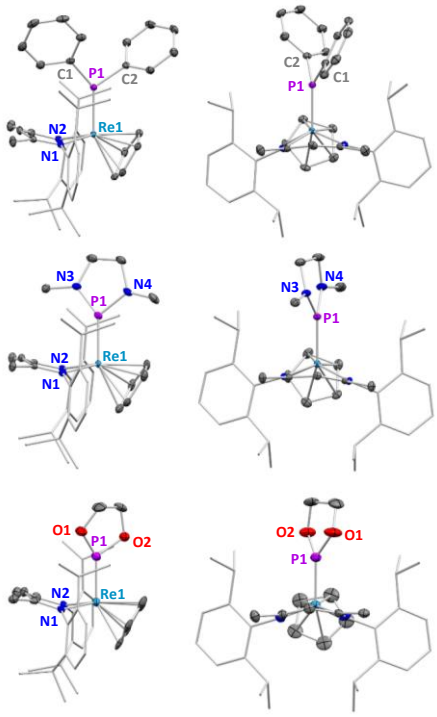

Figure 3. X-ray crystal structures of **2** (top), **3** (middle), and **4** (bottom). The structures are shown in two perspectives and visualized with 50% probability ellipsoids. The BDI aryl groups are shown in wireframe, and hydrogen atoms are omitted for clarity. See Figures S21-S23 for relevant geometric parameters.

lengths and planar geometries at phosphorus clearly indicate XL-type bonding and double bond character for the Re–P bond.[72] The additive covalent radii set forward by Pyykkö are offered as a point of comparison in Table 1.[73] The Re–P bond length in **2** is in excellent agreement with the sum of covalent radii (Σr_{cov}) for a Re–P double bond (2.21 Å). The Re–P bond lengths in **3** and **4** are even shorter than this, implicating a more complex electronic interaction between Re and P. Notably, while the P–C bond lengths in **2** are very close (Δ < 0.01 Å) to Σr_{cov}(P–C), the P–N and P–O bonds in **3** and **4** are roughly 0.1 Å shorter than

their respective Σr_{cov}(P–R), suggesting a considerable P–R π-interaction in these cases.

We observe a clear trend in the Re–P bond lengths of **2**-**4**, with bond length decreasing as the electronegativity of the phosphorus substituent increases. A possible explanation for this phenomenon invokes the negative inductive effect of the R substituents. Increasingly electronegative R substituents withdraw electron density from P, decreasing the radial extent of P s and p orbitals involved in bonding with Re. Conversely, we note that this trend in Re–P bond lengths may be explained by the decrease in the steric profiles of the phosphido moieties. The diphenylphosphido fragment in **2** is larger than the *N*-heterocyclic phosphido fragment **3**, which is itself larger than the *O*-heterocyclic phosphido fragment in **4**.

Phosphido ligands tend to bridge two metal centers when such a configuration is sterically accessible. This is especially true of *O*-substituted phosphido ligands, $P(OR)_2^-$, which tend to be much less sterically inhibited than *N*- or *C*-substituted phosphido ligands. While there are many examples of *bridging* $P(OR)_2^-$ ligands,[74–83] there are only two other crystallographically characterized transition metal complexes with a $P(OR)_2^-$ ligand bonding in a terminal fashion.[48,84] In **2**-**4**, the bulky β-diketiminate ligand plays an important role in preventing dimerization, particularly for complex **4** which contains a rather small *O*-heterocyclic phosphido ligand.

Bonding Analysis of Phosphido Complexes 2-4. To provide further insight into the electronics of the M–P bond in **2**-**4** we turned to density functional theory (DFT) calculations, performing structural optimizations and frequency calculations using the B3PW91 functional. (Computational details may be found in the ESI on page S50.) While simulations of **2** and **3** match the crystallographically determined geometries well, *O*-heterocyclic phosphido complex **4** did not converge to a planar phosphido geometry, as expected (Tables S6-S10). Instead, **4** converges to a bent geometry with a longer Re–P bond length of 2.30 Å and a lower $\Sigma\measuredangle^{P}$ of 326.5°. Including intramolecular dispersion corrections alone did not rectify the discrepancy in geometry. After adding geometry constraints to the P–O distances and P–O–C–H dihedral angles (to mimic the intermolecular C–H···Cp dispersion interactions present in the crystal structure), however, **4** converges to a planar geometry with structural metrics that match the crystallographically determined geometry well. The energetic difference between the unconstrained and constrained simulations of **4** is slight, at only 4.5 kcal/mol. In what follows, computational results reported for **4** refer to the constrained version. To attempt to control for steric differences across **2**-**4**, we also computationally modeled **2′** and **3′**, where **2′** and **3′** contain 5- membered carbon and nitrogen (hetero)cyclic phosphido fragments (PC_4H_8 and ^{H}NHP, respectively) with comparable steric bulk to **4**. Ultimately the optimized geometries and orbital compositions for **2′** and **3′** did not deviate significantly from **2** and **3**, leading us to more confidently ascribe the differences between **2**, **3**, and **4** to the change in phosphorus substituent, and not to steric differences.

A Natural Bond Order (NBO) analysis of **2**-**4** identifies two Re–P bonds for all three complexes, which is corroborated by Re–P Wiberg Bond Indices (WBIs) greater than 1 (Table 2). The first bond is σ-type interaction between a Re s/d hybrid orbital and a P s/p_z hybrid orbital and the second is a π-type interaction between a Re d orbital and a P p_x orbital. Interestingly, altering the electronegativity of the phosphorus substituent simultaneously changes the *hybridization* of the M–P σ-bond and the *polarization* of the M–P π-bond. In all five modeled phosphido complexes, the Re–P σ-bonds are comparably polarized towards P (66-70% P contribution). On the other hand, the π-bond, while approximately covalent in **2** (53.71% P contribution), is polarized towards Re in **3** and **4** (37.24% and 38.77% P contribution, respectively). Consistent with the small R–P–R angles in these complexes, the s character of the phosphorus contribution to the Re–P σ-bond is greater than 50% in all three complexes. This is significantly higher than the 33.3% s character that might be naively expected for a sp^2 hybridization at phosphorus. Notably, as the phosphorus substituent changes from C to N to O, the P component of the σ-bond *increases* in s character, from 51.22% in **2** to 61.44% in **3** to 75.64% in **4**. As the s character of the P orbital increases, the radial extent of this orbital decreases, in part explaining the decrease in bond length from **2** to **3** to **4**.

Table 2. Selected Computational Data on the Re–P σ- and π-Bonding in Complexes 2, 3, and 4.

	Natural Bonding Orbital Contributions			
Complex	Re–P σ		Re–P π	
2	Re (34.1%)	P (65.9%)	Re (46.3%)	P (53.7%)
PR_2 = PPh_2	*s* - 19.4%	*s* - 51.2%	*s* - 0.1%	*s* - 0.1%
	p - 0.2%	*p* - 48.7%	*p* - 0.1%	*p* - 99.8%
	d - 80.4%		*d* - 99.8%	
3	Re (30.8%)	P (69.2%)	Re (62.8%)	P (37.2%)
PR_2 = ^{Me}NHP	*s* - 21.6%	*s* - 61.4%	*s* - 0.1%	*s* - 0.2%
	p - 0.2%	*p* - 38.5%	*p* - 0.1%	*p* - 99.3%
	d - 78.2%		*d* - 99.8%	
4	Re (32.3%)	P (67.7%)	Re (61.2%)	P (38.9%)
PR_2 = OHP	*s* - 20.44%	*s* - 75.64%	*s* - 0.03%	*s* - 0.1%
	p - 0.13%	*p* - 24.26%	*p* - 0.10%	*p* - 99.4%
	d - 79.43%		*d* - 99.88%	

Phosphido complexes **2**-**4** may be conceptually formed from the combination of the metal fragment (BDI)ReCp and the phosphido fragment PR_2. By treating (BDI)ReCp as a L_2MCp type system, three Re–P interactions of varying strength are revealed (Figure 4, *cf.* Figure 1).[38] The strongest of the three is a Re–P σ-interaction, arising from the interaction of the P s/p_z hybrid orbital with the 3a′ orbital of the (BDI)ReCp fragment. The second, comparatively weaker interaction is of π-symmetry and arises from the interaction of the P p_x orbitals with the a_π′ orbital of the (BDI)ReCp fragment. The final (and much weaker) interac-

tion to consider is also of π-symmetry. This interaction involves the P–R σ*-antibonding orbitals and the filled a_π'

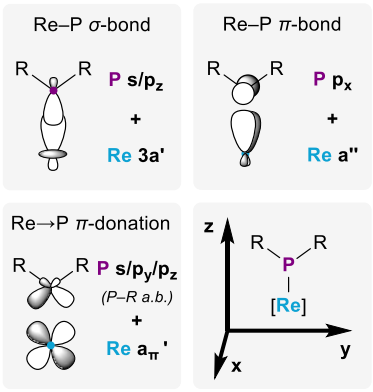

Figure 4. σ- and π-bonding interactions between rhenium and phosphorus in a (BDI)Re(PR_2)Cp type complex.

orbital of the (BDI)ReCp fragment. Importantly, in the L_2MCp system the a_π' orbital is considerably less effective at π-bonding than the a'' orbital.[38] The difference between the a_π' and a'' orbitals (along with steric repulsion from the BDI ligand) explains the observed PR_2 geometries in **2**-**4**. We note that the related *N*-heterocyclic silylene and germylene complexes (BDI)Re(E[PhC(N^{t}Bu)$_2$])Cp (E = Si, Ge) have comparable geometries to phosphido complexes **2**-**4**.[65] While none of these complexes possess a mirror plane, the deviation from mirror symmetry is slight. All possess Cp(centroid)–Re–P–R torsion angles less than 20°, both *in crystallo* and *in silico*.

Crucially, the filled a_σ' and a_π' orbitals in the [(BDI)ReCp]$^+$ fragment are *non-bonding* with respect to the phosphorus p_x orbital, permitting the strong Re–P π-interaction observed in these complexes. The putative donation of the a_π' orbital into two P–R σ* orbitals deserves elaboration. The π-accepting ability of phosphines is now understood to arise from the donation of filled metal d orbitals into P–R σ* orbitals and *not* from the involvement of the 3d orbitals at P.[85] Conceptually, this donation need not be limited to PR_3 ligands and should be present for other phosphorus ligands with polarized P–R σ-bonds such as *N*-heterocyclic phosphido complexes. Indeed, for NHP complex **3** we identified two second order perturbations in the NBO analysis corresponding with weak π-donation from the Re a_π' orbital to the P–N σ* orbitals (9.6/10.3 kcal/mol). While we identified a comparable interaction in **2′** and **3′**, we could not identify such an interaction in **2** and **4**. The absence of this interaction for **2** and **4** is not surprising given how poorly the Re a′ orbital is set up for π-bonding[38] and how weak this interaction is in **2′**, **3**, and **3′**. For **3** and **3′** we also identified more significant second order perturbations, namely π-interactions arising from donation of the p-hybridized NHP N lone pairs to the Re–P π* antibonding orbitals (23.1/21.0 kcal/mol in **3** and 24.9/23.6 kcal/mol in **3′**). The R p → Re–P π* interaction in **3** and **3′** indicates that there may be some degree of delocalization across the Re–P–R π system. Equivalent interactions were not identified for **4**, even though these complexes are structurally similar. This may be attributed to the lower electronegativity of N relative to O, permitting stronger R p → Re–P π* donation. We note that the R p → Re–P π* interaction can be considered to be in competition with the Re d → P–R σ* interaction: the former will shorten the P–R bond and lengthen the M–P bond, while the later will lengthen the P–R bond and shorten the M–P bond. The short P–R distances in **3** and **4** are consistent with the relative strength of these interactions (~23 vs. ~10 kcal/mol for R p → Re–P π* and Re d → P–R σ*, respectively).

A M–PR_2 complex may be considered to be a phosphido complex (arising from the combination of PR_2^- and $[M]^+$) or a phosphenium complex (arising from the combination of PR_2^+ and $[M]^-$), depending on a number of factors. This binary classification is reminiscent of the distinction made between Schrock and Fisher carbenes.[12] We have been unable to demonstrate any productive reactivity of **2**-**4** with alcohols (O–H being the prototypical polarized bond for addition across the M–P bond[86,87]) that might favor the description of these complexes as phosphido or phosphenium complexes. The results of our NBO analysis, along with Re and P natural charge data (see Table S3), suggest that **2** is best described as a planar phosphido complex, while **3** and **4** may be better described as planar phosphenium complexes.

Synthesis and Characterization of a Rhenium Iminophosphanyl Complex. We were interested in synthesizing a metal iminophosphanyl complex as a point of comparison for phosphido complexes **2**-**4**. Pursuing a similar salt metathesis strategy, we combined metalate **1** with one equivalent of iminophosphane Mes*NPCl at low temperature. A rapid color change to dark brown, the evolution of a colorless precipitate, and the ready dissolution of the product in pentane suggested to us that salt metathesis had occurred to yield a neutral product. Spectroscopic and crystallographic data unambiguously confirm the identity of the dark brown product as linear iminophosphanyl complex **5** (Scheme 2).

Scheme 2. Synthesis of Iminophosphanyl Complex 5.

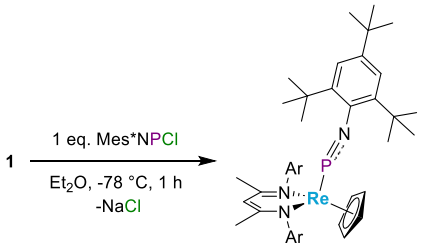

5, 76%

^{1}H NMR signals for the ancillary ligands of **5** fall in the expected regions for a diamagnetic complex and the singlet at +231.5 ppm in the ^{31}P NMR spectrum is as expected for a linear M–PNR geometry. (Bent M–PNR complexes have ^{31}P signals that are significantly downfield, *circa* +700 ppm.[31,88]) The *o*-^{t}Bu groups in the Mes* moiety are inequivalent by ^{1}H and ^{13}C NMR, indicating restricted rota-

Commented [DH1]: footnote

Commented [DH2R1]: Tilley anomalous

tion around the Re–P bond. Single crystal XRD studies reveal a slightly bent iminophosphanyl geometry in **5**: the Re–P–N angle is 161.94(9)° and P–N–C angle is 168.35(19)° (Figure 5). Both the Re–P and P–N distances

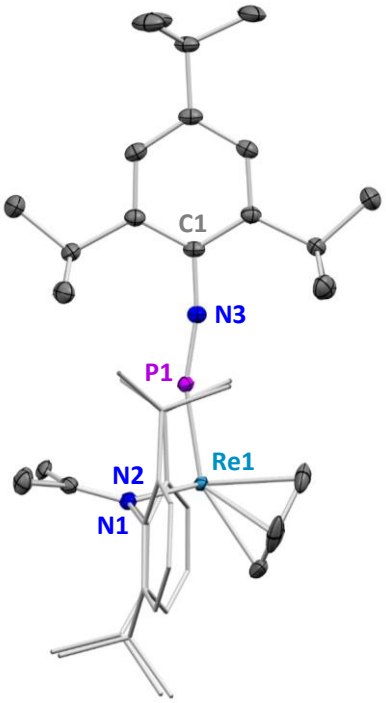

Figure 5. X-ray crystal structure of **5**. The BDI aryl groups are shown in wireframe, hydrogen atoms are omitted for clarity, and ellipsoids are displayed at 50% probability. The complex crystallizes with half an equivalent of *n*-pentane in the outer sphere, which is omitted for clarity.

are quite short, at 2.1374(8) and 1.499(2) Å respectively. For context, the only structurally characterized terminal rhenium phosphide complex has a Re–P distance of 2.0939(6) Å,[89] only marginally shorter than that of iminophosphanyl complex **5**. Interestingly, the parent iminophosphenium ion $[Mes^*N{\equiv}P]^+[AlCl_4]^-$ has a P–N length of 1.475(8) Å,[90] again only marginally shorter than the P–N length in complex **5**. The remarkably short bond lengths prompted us to compare complex **5** with other iminophosphanyl complexes so that we might better conceptualize the electronic and crystallographic structure of this unusual complex.

Only a handful of M–PNR complexes have been reported in the literature. The synthetic routes to these complexes are eclectic: they have been synthesized via silylation of a phosphorus mononitride complex,[91] nitrene transfer to terminal phosphide complexes,[92,93] Cp* shift of a *P*-coordinated RNPCp* complex,[88,94] and salt metatheses of anionic metal complexes with chloroiminophosphanes, RNPCl.[31] Only three M–PNR complexes feature complete crystallographic characterization: the bent iron complex $(CO)_2Fe(PNMes^*)Cp^*$, the related bent ruthenium complex (IPr)(CO)Ru(PNTs)Cp* and the linear molybdenum complex $(N_3N)Mo(PNSiMe_3)$ (Figure 6).[31,92,93] In the iron and

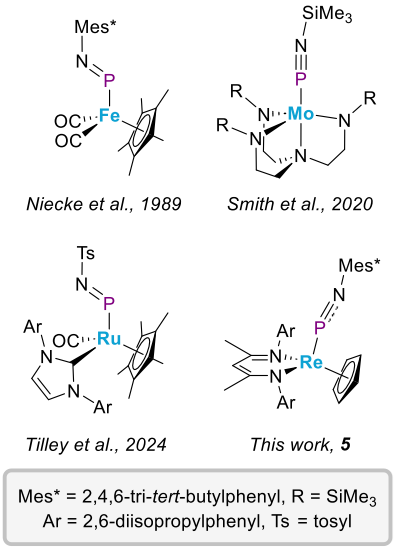

Figure 6. Crystallographically characterized literature iminophosphanyl complexes.

Table 3. Selected Structural and Spectroscopic Data for Iminophosphanyl Complexes Presented Above.

	$(CO)_2Fe(PNMes^*)Cp^*$	$(N_3N)Mo(PNSiMe_3)$
M–P (Å)	2.205(5)	2.138(11) Å
P–N (Å)	1.564(12)	1.514(2)
M–P–N (°)	115.4(5)	177.37(10)
P–N–R (°)	119.8(9)°	161.22(17)
^{31}P (δ)	+787	+199
	(CO)(IPr)Ru(PNTs)Cp*	(BDI)Re(PNMes*)Cp
M–P (Å)	2.24399(3)	2.1374(8)
P–N (Å)	1.603677(13)	1.499(2)
M–P–N (°)	113.0513(7)	161.94(9)
P–N–R (°)	124.0231(6)	168.35(19)
^{31}P (δ)	+234*	+232

The Pyykkö Σr_{cov} for Fe–P (single/double), Mo–P (double/triple), and Ru–P (single/double) are 2.27 Å/2.11, 2.23 Å/2.07 Å, and 2.36 Å/2.16 Å, respectively. See Table 1 for Re–P and P–N Σr_{cov}. *This ^{31}P shift is anomalously shielded for a bent M–PNR complex. This is not commented on in ref. 93.

ruthenium complexes, the M–P distances are between their respective single and double bond Σr_{cov}, and the P–N

distances are consistent with short P–N double bonds (Table 3). The Mo–P and P–N distances in the linear molybdenum complex are quite remarkable; the Mo–P distance lies between the Mo=P and Mo≡P Σr_{cov} and the short P–N distance is closer to the P≡N Σr_{cov} than the P=N Σr_{cov}. As with the molybdenum complex, the Re–P distance of Å in **5** lies between the Re=P and Re≡P Σr_{cov} and the P–N distance is close to the P≡N Σr_{cov}. Clearly, **5** more closely resembles the linear molybdenum complex than the bent iron and ruthenium complexes, though there is a noteworthy difference between **5** and $(N_3N)Mo(PNSiMe_3)$. Even though the iminophosphanyl moiety in $(N_3N)Mo(PNSiMe_3)$ is closer to linearity than in **5**, the P–N distance in the molybdenum complex is somewhat longer than in **5**. We cautiously ascribe the discrepancy in the P–N distances between these two complexes to the superior π-backbonding ability of molybdenum fragment. While in $[(BDI)ReCp]^-$ the a'' orbital is better suited for π-donation than the a_π' orbital, the two orbitals capable of π-bonding in $[(N_3N)Mo]^-$ are necessarily degenerate.

Bonding Analysis of Complex 5 and its First Row Analogues. Like their nitrosyl analogues, iminophosphanyl complexes feature nuanced metal-ligand bonding interactions. Borrowing a common convention from metal nitrosyl chemistry, complex **5** can be represented in Enemark-Feltman notation as a $\{RePNR\}^6$ complex.[95] This suggests that the linear Re–P–N geometry in **5** is electronically favored (and not merely a consequence of steric effects). To better understand the bonding along the Re–P–N axis in **5** we turned to computational methods, performing structural optimizations and frequency calculations on complex **5** using DFT. Given the novelty of iminophosphanyl complex **5**, we decided to compare **5** with its first-row nitrosyl, diazenido, and siloxycarbyne analogues so that we might better contextualize our computational results. While the nitrosyl complex analogous to **5** (*i.e.* (BDI)Re(NO)Cp, **5-NO**) has not been reported, we previously synthesized and characterized the related diazenido and siloxycarbyne complexes, (BDI)Re(NNSiMe$_3$)Cp (**5-NNSiMe$_3$**) and (BDI)Re(COSiMe$_3$) (**5-COSiMe$_3$**).[62] A detailed crystallographic and computational comparison of **5**, **5-NNSiMe$_3$**, **5-COSiMe$_3$**, and **5-NO** may be found in the Supporting Information (See pages S41-43), but the principle findings are summarized below. The Re–X1–X2 geometries of these four complexes are similar to each other, both *in crystallo* and *in silico*. The P–N bond in **5** is significantly more polarized (towards N) than the analogous X1–X2 bonds in **5-NNSiMe$_3$**, **5-COSiMe$_3$**, and **5-NO**. While **5-NNSiMe$_3$** and **5-NO** are a good analogy for **5** in terms of the relative strengths of π-bonding between Re–X1 and X1–X2, **5-COSiMe$_3$** is a (slightly) better analogy for **5** in terms of bond polarization. For complex **5** the pseudolinear geometry and natural charge data (Re: +0.11, P: +1.05, and N: –0.97, Table S3), lead us to conclude that **5** has considerable iminophosphenium character. We note that the Re–P WBI and natural charges for iminophosphanyl complex **5** (WBI: 1.36, Re: +0.11, P: +1.05) are remarkably similar to those of *N*-heterocyclic phosphido complex **3** (WBI: 1.36, Re: +0.16, P: +1.33). Therefore, we believe that these species should be described in a similar manner, that is, if **3** is considered an *N*-heterocyclic phosphenium complex then **5** should likewise be considered an iminophosphenium complex.

Synthesis and Characterization of a Rhenium Phosphinidene Complex. To expand on the comparisons drawn between **2**, **3**, **4**, and **5** we sought to synthesize a phosphinidene complex from metalate **1**. We were particularly interested in this pursuit, as there is only one example of a metal fragment for which the iminophosphanyl and phosphinidene complexes have both been isolated, namely the iron fragment $(CO)_2FeCp^*$. In 1984 Gladysz et al. reported spectroscopic evidence for $[(CO)_2Fe(PN^iPr_2)Cp^*][AlCl_4]$ at low temperature, but were unable to isolate this product, hypothesizing that it was thermally unstable.[29] In 1989 Niecke et al. reported the iminophosphanyl complex $(CO)_2Fe(PNMes^*)Cp^*$ and characterized it by X-ray diffraction.[31] Later, in 2003, Carty et al. demonstrated that Gladysz's iron phosphinidene complex was indeed stable at room temperature under rigorous exclusion of water and characterized it by X-ray diffraction.[30] We anticipated that a cationic phosphinidene complex $[(BDI)Re(PR)Cp]^+$ would feature a strong Re–P double bond, offering an interesting complement to $[(CO)_2Fe(PN^iPr_2)Cp^*]^+$, which has minimal Fe–P π-bonding.

As a potential route to this class of complex, we reinvestigated the reaction of **1** with dichlorophosphines ($PRCl_2$), which previously yielded the chloride complex (BDI)Re(Cl)Cp as the major product. One conceivable pathway to (BDI)Re(Cl)Cp in these reactions is through a chlorophosphido intermediate, (BDI)Re(PRCl)Cp, which subsequently collapses to (BDI)Re(Cl)Cp and phosphinidene, PR. We note that the isolobal chlorophosphido complexes, $(CO)_2Mo(PRCl)Cp$, are stable and have been crystallographically authenticated (R = 2,2,6,6-tetramethylpiperidine[52] or Mes*[96]). We performed a low temperature addition of **1** to one equivalent of $PCl_2N^iPr_2$ in the presence of one equivalent of a halide abstraction reagent ($AlCl_3$, $GaCl_3$, $NaBPh_4$, LiTFSI, $TFSI^-$ = $[N(CF_3SO_2)_2]^-$) with the intention of intercepting the putative chlorophosphido complex $(BDI)Re(PClN^iPr_2)Cp$. Soon after addition, the reaction mixture turned a dark brown, in contrast to the red coloration previously observed in corresponding reactions without a halide abstraction reagent. Workup of the dark brown reaction mixture provided moderate yields of dark green crystals that were identified as cationic terminal phosphinidene complex $[(BDI)Re(PN^iPr_2)Cp][\mathbf{X}]$ (**6-X**) (**X** = $AlCl_4^-$, $GaCl_4^-$, BPh_4^-, $TFSI^-$, Scheme 3). Complexes **6-X** display characteristic downfield ^{31}P resonances around +712 ppm with minor variations (<10 ppm) depending on the counterion, temperature, and solvent (Figure S15). No new products could be isolated from analogous reactions with PCl_2Ph, hinting that the amido substituent at phosphorus may serve to stabilize the product and/or a reactive intermediate.

The ^1H NMR spectrum of **6-BPh$_4$** in CD_2Cl_2 collected at ambient temperature shows *one* doublet integrating to 12H and *one* septet integrating to 2H associated with the phosphinidene isopropyl methyl and methine groups, respectively. We performed variable temperature (VT) NMR studies on **6-BPh$_4$** to see if the signals for the phosphinidene isopropyl groups could be resolved at low temperature. Indeed, upon cooling from 298 K to 223 K the

isopropyl methyl peak transitions from one doublet to two doublets and the isopropyl methine peak transitions from one broad singlet to two broad singlets (Figures S18 and S19). Using the coalescence temperatures for these transitions we determined the free energy barrier to rotation around the P–N bond in **6-BPh$_4$** to be 12.1(5) and 11.8(5) kcal/mol at 248 and 260 K, respectively. (See ESI S26-S27 for relevant calculations.) A recently reported ruthenium dimethylaminophosphinidene complex is, to our knowledge, the only other aminophosphinidene complex with rapid rotation around the P–N bond at room temperature.[97] The observation of a single methyl peak at room temperature sets a rough upper limit of 13 kcal/mol for the barrier of rotation around the P–N bond in this complex. Besides these two complexes, all terminal aminophosphinidene complexes in the literature feature restricted rotation around the P–N bond at room temperature.[30,98–102] This establishes a barrier of rotation around the P–N bond of >15 kcal/mol in these complexes, substantially higher than 12 kcal/mol barrier for **6-BPh$_4$**. The molybdenum aminophosphinidene complex [Cp*Mo(PN^{i}Pr$_2$)(CO)$_3$][AlCl$_4$], for example, maintains two distinct ^{i}Pr methyl and methine resonances up to 60 °C,[98] setting a lower limit of approximately 17 kcal/mol for the barrier to P–N rotation in this complex.

Scheme 3. Synthesis of Phosphinidene Complex 6-X.

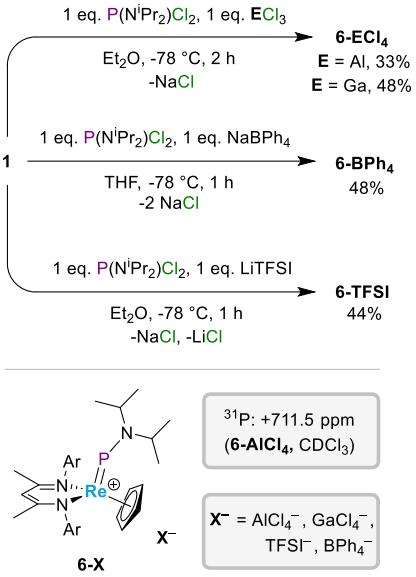

Crystallographic studies of **6-TFSI** undertaken at 100 K reveal short Re–P and P–N distances of 2.2056(10) and 1.641(3) Å, respectively (Figure 7). The phosphinidene amido unit is planar, with a $\Sigma\angle_N$ of 360.0°. Furthermore, the low Re–P–N–C torsion angle of 7.5(4)° implies some degree of conjugation between the Re–P and P–N π-interactions. A survey of the literature reveals that **6-TFSI** possesses a substantially shorter M–P distance than related aminophosphinidene complexes. An illustrative example is [(CO)$_5$Re(PN^{i}Pr$_2$)]AlCl$_4$, which has a Re–P distance of 2.446(3) Å.[103] The Re–P distance in **6-TFSI** is more than 0.2 Å shorter at 2.2056(10) Å. Clearly, replacing π-accepting ligands with strongly σ-donating ligands results in a decrease in the M–P bond length and an increase in the P–N bond length. The comparison, however, between **6-TFSI**

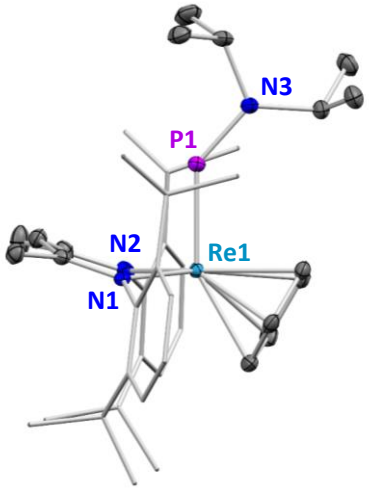

Figure 7. X-ray crystal structure of **6-TFSI**. The BDI aryl groups are shown in wireframe, hydrogen atoms are omitted for clarity, and ellipsoids are displayed at 50% probability. The complex crystallizes with two and a half equivalents of THF and a TFSI counterion in the outer sphere, which are omitted for clarity.

and [(CO)$_5$Re(PN^{i}Pr$_2$)]AlCl$_4$ is not perfect due to the difference in oxidation states between the two compounds (5+ vs. 3+). In 2007 Carty and coworkers published an elegant study of terminal molybdenum aminophosphinidene complexes with varying ancillary ligands (Figure 8).[104] Therein, Carty et al. demonstrate that the sequential replacement of π-accepting carbon monoxide ligands from [Cp*Mo(PN^{i}Pr$_2$)(CO)$_3$]AlCl$_4$ with strongly σ-donating phosphine ligands *decreases* the M–P bond length and *slightly increases* the P–N bond distance. In their work, Carty et al. justify this trend by arguing that the replacement of CO ligands with phosphines increases the electron density at the metal center, thus increasing "metal to phosphinidene π-back-donation" and shortening the phosphinidene M–P distance. Correspondingly, Carty continues, the increase in M→P π-back-donation diminishes N→P π donation and lengthens the P–N bond. This competition, so to speak, between M→P π-donation and N→P π-donation in aminophosphinidene complexes has been demonstrated in a number of computational studies.[13,105–109]

Bonding Analysis of Phosphinidene Complex 6$^+$. We employed DFT calculations to further investigate the M–P–N π-interactions in **6**$^+$. Optimization of **6**$^+$ provides a structure that matches the crystallographically determined geometry well (Table S15). NBO analysis of **6**$^+$ identifies two

interactions between Re and P (Table S3). The first is a covalent σ-interaction (Re: 51.5%, P: 48.5%) and the second is a π-interaction polarized towards rhenium (Re: 73.5%, P: 26.5%). The polarization of the π-interaction towards rhenium is suggestive of a singlet character for the phosphinidene moiety and is consistent with competition from the p hybridized lone pair at nitrogen. In

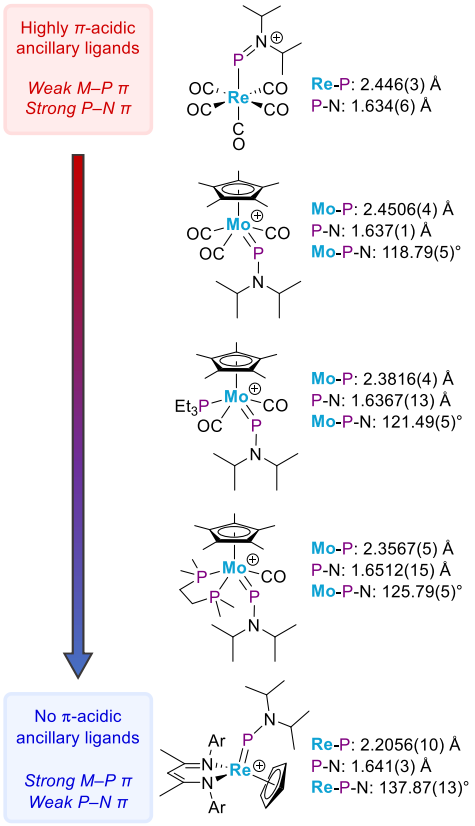

Figure 8. Structural comparison of phosphinidene complex **6-TFSI** with related molybdenum and rhenium phosphinidene complexes $[Re(PN^iPr_2)(CO)_5]^+$,[103] $[Mo(PN^iPr_2)(CO)_3Cp^*]^+$,[98] $[Mo(PN^iPr_2)(CO)_2(PEt_3)Cp^*]^+$,[104] and $[Mo(PN^iPr_2)(CO)(\kappa_2\text{-dmpe})Cp^*]^+$.[104]

addition to a 2-electron P–N σ-interaction polarized towards nitrogen (P: 22.6%, N: 77.4%) we identify a 3-center, 4-electron hyperbond between the nitrogen lone-pair and the Re–P π-bond (Table S4). This conjugation of Re–P and P–N π-interactions is consistent with the coplanar geometry of the phosphinidene fragment we observe in the XRD-determined and DFT-simulated structures of **6**$^+$. Analysis of WBIs supports the VT-NMR results indicating that the Re–P π-interaction is stronger than the P–N π-interaction. The WBI of the Re–P bond is 1.39 (comparable to phosphido complexes **2**, **3**, and **4**), while the WBI of the P–N bond is 1.00. (For context, this is higher than the WBI of 0.76 for the P–N bond in **3**, but lower than the WBI of 1.36 the P–N bond in **5**.) Notably, while the P contribution to the Re–P σ-bond in **2**, **3**, and **4** has a much higher s character than might be expected for a sp^2 hybridization, the P contribution to the Re–P σ-bond in **6**$^+$ has a much higher p character than might be expected for a sp^2 hybridization. In the Re–P σ-bond of **6**$^+$ the P contribution is 10.8% s character and 88.7% p character. Correspondingly, the P lone pair is primarily s character (s: 77.74%, p: 22.2%).

To minimize confusion in this paper, **6**$^+$ is drawn with a covalent rhenium-phosphorus double bond (*i.e.* as a triplet phosphinidene), but we acknowledge that a σ-dative, π-retrodative Re–P bond (*i.e.* a singlet phosphinidene) is a valid alternative description of the bonding in complex **6**$^+$. For those with interest in how phosphinidene complexes are drawn, we have written an appendix on the matter which can be found in the supporting information (S44).

Synthesis and Structural Analysis of a Radical Phosphinidene Complex. In addition to terminal phosphinidene complex **6-X**, we were also interested in synthesizing the terminal phosphide complex (BDI)Re(≡P)Cp analogous to the terminal nitride complex (BDI)Re(≡N)Cp previously reported by our group.[61] In the previously reported synthesis of (BDI)Re(≡N)Cp, paramagnetic (BDI)ReCp is combined with an excess of RN_3, resulting in homolytic cleavage of the N–R bond and a formal three-electron oxidation of the metal center. We theorized that (BDI)Re(≡P)Cp might be accessible from **6-X** through a similar process (*i.e.* homolytic cleavage of the P–N bond). Anticipating that over-reduction of **6-X** would lead back to anionic complex **1**, we turned to the relatively mild one-electron reductant cobaltocene. The low temperature combination of dark green **6-X** and purple $CoCp_2$ in THF resulted in minimal color change. During workup, however, the hexane extract readily took on a green-amber coloration and orange powdery solids were filtered out, consistent with the reduction of **6-X** to a neutral product and the oxidation of $CoCp_2$ to $[CoCp_2]X$. ^1H NMR revealed the green-amber product to be paramagnetic, inconsistent with an assignment of (BDI)Re(≡P)Cp. Crystallographic efforts unequivocally confirmed the assignment of the dark green-amber product as the neutral, paramagnetic, terminal phosphinidene complex (BDI)Re(PN^iPr_2)Cp (**6**$^\bullet$, Scheme 4). While there are several known examples of

Scheme 4. Synthesis of Phosphinidene Complex 6$^\bullet$.

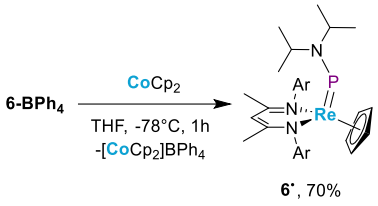

bridging paramagnetic phosphinidene species,[110–115] there are, to our knowledge, only two other terminal paramagnetic phosphinidene complexes that have been structurally authenticated.[116] These vanadium (IV) species,

(BDI)$V^{IV}(CH_2{}^tBu)$(=PAr) (Ar = 2,4,6-$^iPr_3C_6H_2$ and 2,4,6-$^tBu_3C_6H_2$), were noted to decompose over several hours at room temperature in solution or in the solid state. Complex **6•**, on the other hand, can be stored at room temperature for several months with minimal decomposition, provided that the sample is kept rigorously air- and water-free. We note that excess cobaltocene is unable to effect the cleavage of the P–N bond. Our attempts to reduce **6•** with more powerful reducing agents gave intractable mixtures of products.

Crystallographic analysis of **6•** reveals a lengthening of the Re–P and P–N bonds relative to **6-TFSI** (to 2.2632(8) and 1.683(3) Å, respectively) as expected with increased electron-electron repulsion (Figure 9). The Re–P–N–R

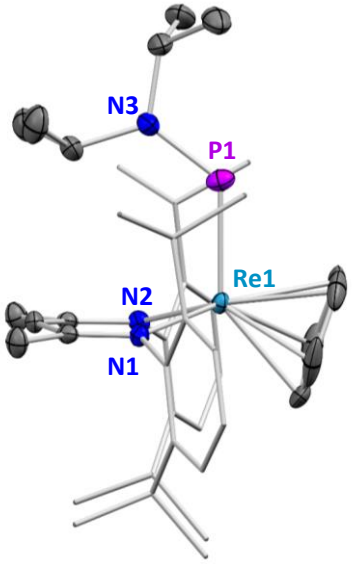

Figure 9. X-ray crystal structure of **6•**. The BDI aryl groups are shown in wireframe, hydrogen atoms are omitted for clarity, and ellipsoids are displayed at 50% probability.

torsion angle and Re–P–N angles are lower in **6•** than in **6-TFSI**, at 2.9(3)° and 127.94(9)°, respectively. Perhaps most remarkably from a structural standpoint, the phosphinidene amido substituent in **6•** has 'flipped over' phosphorus relative to **6-TFSI**. We cannot confidently ascribe a cause to this geometric difference.

Characterization of Complex 6• by Electron Paramagnetic Resonance Spectroscopy. The valence configuration of rhenium in **6•** is $5d^3$, giving two possibilities for the spin state, S = 1/2 and S = 3/2. The effective magnetic moment, μ_{eff}, of **6•** is calculated to be 1.64 μ_B by the Evans method (Figure S20), consistent with a spin state of S = 1/2. (The spin-only magnetic moment, μ_{so}, is 1.73 μ_B for a S = 1/2 complex and 3.87 μ_B for a S = 3/2 complex.) It is uncommon to observe a spin state of S = 1/2 for a complex of Re^{IV}, as octahedral field splitting typically leads to spin states of S = 3/2 (t_{2g}^3).[117–123] The homoleptic, tetrahedral aryl complex $Re^{IV}(o\text{-}MeC_6H_4)_4$ and several Re^{IV} PNP pincer complexes serve as rare examples of Re^{IV} complexes with low spin (S = 1/2) configurations.[124,125] Most examples of S = 1/2 d^3 complexes are of Mn^{IV},[126,127] Fe^{V},[128–132] or Mo^{III}.[133–136] Two factors must hold true for a d^3 complex to possess a S = 1/2 ground state: the coordination geometry must deviate from octahedral (to break the degeneracy of t_{2g} set) and the d splitting must be large (such that $\Delta_{d\text{-}d} > E_{pairing}$). We reason that the S = 1/2 spin state of **6•** is attributable to the low symmetry ligand environment which lifts the degeneracy of the 5d orbitals of rhenium.

To further investigate the electronic properties of **6•**, we measured EPR spectra in the X-, Q-, and D-bands (9.4, 34, and 130 GHz, respectively). The X-band continuous wave (CW) EPR spectrum shows a complicated multiline signal centered about $g \sim 2$ featuring both Re (Figure 10A and B, blue) and ^{31}P (I = 1/2) hyperfine interactions (Figure 10A, green). Notably, both magnetic isotopes of rhenium (^{185}Re,

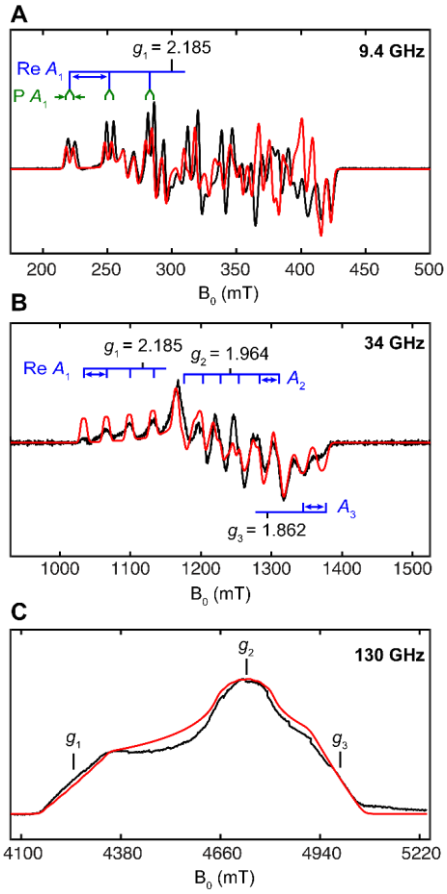

Figure 10. EPR spectra of complex **6•** (black traces) and simulations (red traces) at multiple frequencies. (A) X-band CW EPR spectrum of **6•**. Acquisition parameters: T = 15 K, fre-

quency = 9.4 GHz, microwave power = 0.2 mW, modulation amplitude = 0.5 mT. (B) Pseudomodulated Q-band ESE-EPR spectrum of **6•**. Acquisition parameters: T = 10 K, frequency = 34 GHz, $\pi/2$ pulse = 12 ns, τ = 300 ns, modulation amplitude = 1 mT. (C) D-band ESE-EPR spectrum of **6•**. Acquisition parameters: T = 10 K, frequency = 130 GHz, $\pi/2$ pulse = 45 ns, τ = 300 ns. Additional experimental details on page S40. Where resolvable, Re hyperfine shown in blue and ^{31}P hyperfine shown in green.

37.4% and ^{187}Re, 62.6%) are I = 5/2 with very similar nuclear gyromagnetic ratios; thus, a six-line pattern is expected for pattern is expected for the Re hyperfine interaction. The g-anisotropy is readily resolved in the D-band electron spin-echo detected EPR (ESE-EPR) spectrum (Figure 10C), while Re hyperfine interactions at each g-value can be resolved in the pseudomodulated Q-band ESE-EPR spectrum (Figure 10B, blue). Together, the spectra can be reasonably simulated as an S = 1/2 system with a g-tensor of [2.185, 1.964, 1.862], A Re = [1025, 764, 670] MHz, and A ^{31}P = [160, 226, 195] MHz. The magnitude of the ^{31}P hyperfine interactions in **6•** is much larger than that of the related complex [(BDI)Re^{VI}Cp(*cyclo*-P$_3$)]$^+$ (a_{iso} = 6 MHz),[61] but is comparable to that of the vanadium phosphinidene complex (BDI)V^{IV}(CH$_2$^{t}Bu)(=PAr) (a_{iso} ≈ 40 G, or ≈ 112 MHz).[116] This result is consistent with higher covalency between the metal center and the phosphinidene moiety than the *cyclo*-P$_3$ group. Further analysis of the A ^{31}P tensor of **6•** via decomposition into isotropic (a_{iso} = 194 MHz) and anisotropic ([-34, 32, 1] MHz) terms reveals a small spin density on the P 3s orbital of~0.01 using a_0 = 13306 MHz for one unpaired electron on the P 3s orbital.[137] Utilizing a spin density of ρ_{Re} ≈ 0.64 (DFT) and a Re–P bond distance of 2.26 Å (XRD) a small nonlocal dipolar coupling value of ~1.8 MHz can be estimated which arises from the through-space electron-nuclear dipole interactions. The remaining local dipolar coupling term estimates ~0.08 spin density on the P 3p orbitals. Together, this analysis estimates a combined (3s + 3p) spin density of ~ 0.09 on P. The simulated g, A Re, and A ^{31}P tensors and the estimated spin density on P are close to predicted values from DFT (g = [2.22, 2.05, 1.94], A Re = [1485, 1228, 967] MHz, A ^{31}P = [165, 164, 221] MHz, ρ_P = 0.06).

DFT calculations indicate that the spin density in **6•** is largely concentrated in a d orbital at Re (Figure 11). This orbital bears a striking resemblance to the a_π' orbital in the L_2MCp system. The weakening of the Re–P and P– N bonds (as evidenced in the crystal structure) is corroborated by a decrease in the WBIs from **6**$^+$ (Re–P:1.39, P–N: 1.00) to **6•** (Re–P: 1.24, P–N: 0.93). While the Re–P σ-bond in **6**$^+$ is covalent (Re: 51.5%, P: 48.5%), the Re–P σ-bond in **6•** is polarized towards phosphorus (Re: 36.5%, P: 63.5%) (Table S3). Correspondingly, the natural charge at phosphorus decreases from +0.83 in **6**$^+$ to +0.48 in **6•**. Even though the radical in **6•** is centered at the metal, the electron density in the Re–P σ-bond has shifted towards phosphorus such that the natural charge at rhenium remains almost entirely unchanged (+0.29 in **6**$^+$, +0.29 in **6•**).

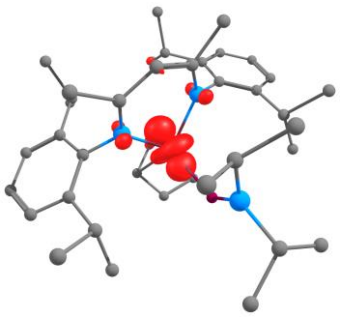

Figure 11. Spin density plot of **6•**. The isosurface value is 0.0518.

CONCLUSIONS

By employing a metal fragment capable of forming strong π-interactions and a bulky ligand set capable of sterically protecting reactive species we were able to isolate and fully characterize an array of six Re–P multiply bonded complexes. *N*- and *O*-heterocyclic phosphido complexes **3** and **4** possess distinct structural and electronic properties that distinguish them from diphenylphosphido complex **2**, highlighting the considerable influence of the phosphorus substituent on the length and polarization of the M–P bond. Complex **5**, featuring exceptionally short Re–P and P–N bonds, is notable for being the second crystallographically characterized example of an iminophosphanyl complex binding in the linear "iminophosphenium mode." Cationic phosphinidene complex **6**$^+$ is a rare example of an aminophosphinidene with a strong M–P π interaction and a weak P–N interaction, which prompted us to reevaluate the criteria for the categorization of phosphinidene complexes as 'nucleophilic' and 'electrophilic.' The surprising stability of radical phosphinidene complex **6•** further demonstrates the remarkable ability of this rhenium system to support unusual bonding motifs and stabilize reactive species across the periodic table. The d^4 [(BDI)ReCp]$^+$ fragment now serves as the second example of a metal fragment for which phosphido, iminophosphanyl, and phosphinidene complexes have all been fully characterized.

ASSOCIATED CONTENT

Experimental procedures, NMR data, crystallographic data, EPR parameters, supplementary discussion, and computational details. This material is available free of charge via the Internet at http://pubs.acs.org.

Accession Codes

CCDC 2340739-2340744 contain the supplementary crystallographic data for this paper. These data can be obtained free of charge via www.ccdc.cam.ac.uk/data_request/cif or by emailing data_request@ccdc.cam.ac.uk, or by contacting The Cambridge Crystallographic Data Centre, 12 Union Road, Cambridge CB2 1EZ, UK; fax: +44 1223 336033.

AUTHOR INFORMATION

Corresponding Author

John Arnold – *Department of Chemistry, University of California, Berkeley, California 94720, United States;* 0000-0001-9671-227X, Email: arnold@berkeley.edu

Authors

David Hales – *Department of Chemistry, University of California, Berkeley, California 94720, United States;* 0009-0007-1743-3725

Thayalan Rajeshkumar – *LPCNO, Université de Toulouse, INSA Toulouse, 135 Avenue de Rangueil, Toulouse 31077, France;* 0000-0001-5109-8093

Angela A. Shiau – *Department of Chemistry, University of California, Davis, California 95616, United States;* 0000-0003-4395-9847

Guodong Rao – *Department of Chemistry, University of California, Davis, California 95616, United States;* 0000-0001-8043-3436

Erik Ouellette – *Department of Chemistry, University of California, Berkeley, California 94720, United States;* 0000-0003-2138-6259

Robert G. Bergman – *Department of Chemistry, University of California, Berkeley, California 94720, United States;* 0000-0002-3105-8366

R. David Britt – *Department of Chemistry, University of California, Davis, California 95616, United States;* 0000-0003-0889-8436

Laurent Maron – *LPCNO, Université de Toulouse, INSA Toulouse, 135 Avenue de Rangueil, Toulouse 31077, France;* 0000-0003-2653-8557

Author Contributions

D.P.H. carried out synthetic work, collected NMR, MP, and EA data, generated figures (with the exception of EPR and DFT figures), and drafted the manuscript. T.R. performed DFT calculations, generated DFT figures, and assisted in writing sections on DFT. A.A.S., G.R., and R.D.B. collected EPR data, generated EPR figures, and wrote sections on EPR. E.T.O. collected and processed XRD data. R.G.B., R.D.B., L.M., and J.A. supervised and directed the study. All authors have analyzed the results, commented on, and given approval to the final version of the manuscript.

ACKNOWLEDGMENT

This research was funded by the NSF (Grant No. 1954612 to J.A. and R.G.B.). EPR spectroscopy was supported by the NIH (Grant No. 2R35GM126961 to R.D.B). The authors thank Dr. Hasan Celik and UC Berkeley's NMR facility in the College of Chemistry (CoC-NMR) for spectroscopic assistance. Instruments in the CoC-NMR are supported in part by the NIH (Grant No. S10OD024998). L.M. is a senior member of the Institut Universitaire de France. CalMip is acknowledged for a generous grant of computing time. Prof. Simon Humphrey (University of Texas, Austin) is thanked for a generous donation of rhenium. Dr. Michael Boreen, Dr. Jade Fostvedt, I. Joe Brackbill, Chris Ye, and Sheridon Kelly are thanked for helpful discussions.

REFERENCES

(1) Vaska, L.; DiLuzio, J. W. Carbonyl and Hydrido-Carbonyl Complexes of Iridium by Reaction With Alcohols. Hydrido Complexes by Reaction with Acid. *J. Am. Chem. Soc.* **1961**, *83* (12), 2784–2785. https://doi.org/10.1021/ja01473a054.

(2) Vaska, L. Reversible Activation of Covalent Molecules by Transition-Metal Complexes. The Role of the Covalent Molecule. *Acc. Chem. Res.* **1968**, *1* (11), 335–344. https://doi.org/10.1021/ar50011a003.

(3) Osborn, J. A.; Jardine, F. H.; Young, J. F.; Wilkinson, G. The Preparation and Properties of Tris(Triphenylphosphine)Halogenorhodium(I) and Some Reactions Thereof Including Catalytic Homogeneous Hydrogenation of Olefins and Acetylenes and Their Derivatives. *J. Chem. Soc.* **1966**, 1711–1732.

(4) Trnka, T. M.; Grubbs, R. H. The Development of L2X2Ru=CHR Olefin Metathesis Catalysts: An Organometallic Success Story. *Acc. Chem. Res.* **2001**, *34* (1), 18–29. https://doi.org/10.1021/ar000114f.

(5) Tolman, C. A. Steric Effects of Phosphorus Ligands in Organometallic Chemistry and Homogeneous Catalysis. *Chem. Rev.* **1977**, *77* (3), 313–348. https://doi.org/10.1021/cr60307a002.

(6) Lagasse, F.; Kagan, H. B. Chiral Monophosphines as Ligands for Asymmetric Organometallic Catalysis. *Chem. Pharm. Bull.* **2000**, *48* (3), 315–324.

(7) Fey, N.; Orpen, A. G.; Harvey, J. N. Building Ligand Knowledge Bases for Organometallic Chemistry: Computational Description of Phosphorus(III)-Donor Ligands and the Metal-Phosphorus Bond. *Coord. Chem. Rev.* **2009**, *253* (5–6), 704–722. https://doi.org/10.1016/j.ccr.2008.04.017.

(8) Hartwig, J. F. Organotransition Metal Chemistry: From Bonding to Catalysis; 2010; pp 33–41.

(9) Waterman, R. Metal-Phosphido and -Phosphinidene Complexes in P–E Bond-Forming Reactions. *Dalt. Trans.* **2009**, *9226* (1), 18–26. https://doi.org/10.1039/b813332h.

(10) Mathey, F.; Duan, Z. Activation of A-H Bonds (A = B, C, N, O, Si) by Using Monovalent Phosphorus Complexes [RP→M]. *Dalt. Trans.* **2016**, *45* (5), 1804–1809. https://doi.org/10.1039/c5dt02532j.

(11) Wen, Q.; Feng, B.; Chen, Y. Rare-Earth Metal Phosphinidene Complexes: A Trip from Bridging One to Terminal One. *Acc. Chem. Res.* **2023**, *56* (23), 3343–3357. https://doi.org/10.1021/acs.accounts.3c00429.

(12) Rosenberg, L. Metal Complexes of Planar PR2 Ligands: Examining the Carbene Analogy. *Coord. Chem. Rev.* **2012**, *256* (5–8), 606–626. https://doi.org/10.1016/j.ccr.2011.12.014.

(13) Ehlers, A. W.; Lammertsma, K.; Baerends, E. J. Phosphinidene Complexes M(CO)5-PR: A Density Functional Study on Structures and Electronic States. *Organometallics* **1998**, *17* (13), 2738–2742. https://doi.org/10.1021/om980057i.

(14) Slootweg, J. C.; Lammertsma, K. Product Class 1: Phosphinidenes and Terminal Phosphinidene Complexes. In *Science of Synthesis*; 2013; pp 15–26. https://doi.org/10.1055/sos-sd-042-00002.

(15) Barrow, M. J.; Sim, G. A. Metal-Carbonyl and Metal-Nitrosyl Complexes. Part XVI. Comparison of the Molecular Structures of Dicarbonyl(π-Cyclopentadienyl)[Bis-(Trifluoromethyl)Phosphino]Iron, [(π-C5H5)Fe(CO)2P(CF3)2], and Its Oxidation Product, [(π-C5H5)Fe(CO)2P(:O)(CF3)2]. *J.C.S. Dalt.* **1975**, 291–295.

(16) Hutchins, L. D.; Duesler, E. N.; Paine, R. T. Structure and Bonding in a Phosphenium Ion-Iron Complex, Fe[H5-(CH3)5C5](CO)2[PN(CH3)CH2CH2NCH3]. Demonstration of Phosphenium Ion Acceptor Properties. *Organometallics* **1982**, *1*, 1254–1256.

(17) Weber, L.; Kaminski, O.; Stammler, H.-G.; Neumann, B.; Boese, R. Übergangsmetall-Substituierte Acylphosphane Und Phosphaalkene, 24 Dipolare [3+2]- Und [2+2]-Cycloadditionen von Carbonyl-Aktivierten Alkinen an (H5-C5Me5)(CO)2Fe-P=C(NMe2)2. *Zeitschrift für Naturforsch.* **1994**, *49b*, 1693–1706.

(18) Weber, L.; Kleinebekel, S.; Pumpenmeier, L.; Stammler, H. G.; Neumann, B. Fumarodinitrile: A Versatile Reagent in Phosphaalkene and Arsaalkene Chemistry. *Organometallics* **2002**, *21* (9), 1998–2005. https://doi.org/10.1021/om010990c.

(19) Kubo, K.; Kawanaka, T.; Tomioka, M.; Mizuta, T. Synthesis

and Crystal Structures of P-Iron-Substituted Phosphinoborane Monomers. *Organometallics* **2012**, *31* (5), 2026–2034. https://doi.org/10.1021/om201287s.

(20) Xin, T.; Geeson, M. B.; Zhu, H.; Qu, Z. W.; Grimme, S.; Cummins, C. C. Synthesis of Phosphiranes via Organoiron-Catalyzed Phosphinidene Transfer to Electron-Deficient Olefins. *Chem. Sci.* **2022**, *13* (43), 12696–12702. https://doi.org/10.1039/d2sc05011k.

(21) Weber, L.; Reizig, K.; Boese, R. (Phosphinocarbonyl)Eisen-Komplexe – Eine Neuartige Komplexklasse. *Chem. Ber.* **1985**, *118*, 1193–1203. https://doi.org/10.1002/cber.19851180335.

(22) Angerer, W.; Malisch, W.; Norman, N. C.; Cowley, A. H. Dicarbonyl(H5-Pentamethylcyclopentadienyl)Ferrio(t-Butyl)Chlorophosphine: A Metallo-Phosphine Exhibiting Multifaceted Reactivity. *J. Chem. Soc., Chem. Comm.* **1985**, 1811–1812.

(23) Mcnamara, W. F.; Reisacher, H. U.; Duesler, E. N.; Paine, R. T. Synthesis and Alkylation of an Iron Phosphane Complex. Crystal and Molecular Structure Determinations for CpFe(CO)2{P(C6H5){N[Si(CH3)3]2}} and CpFe(CO)2{P(CH3)(C6H5){N[Si(CH3)3]2+}}(O3SCF3-). *Organometallics* **1988**, *7* (6), 1313–1317. https://doi.org/10.1021/om00096a013.

(24) Brombach, H.; Niecke, E.; Nieger, M. Synthetic Routes to the First P-Metalated Phosphiranes: Synthesis and Structure of (H5-Cyclopentadienyl)Dicarbonyl[2,2,3-Tris(Trimethylsilyl)-1λ3-Phosphacyclopropyl]Iron. *Organometallics* **1991**, *10* (12), 3949–3951. https://doi.org/10.1021/om00058a002.

(25) Weber, L.; Sonnenberg, U.; Stammler, H. G.; Neumann, B. Synthese Und Struktur von H1-2,4-Diaza-3-Phosphapenta-1,4-Dien-3-Yl-Komplexen Des Eisens Und Rutheniums. *Zeitschrift für Naturforsch.* **1991**, *46b*, 714–718.

(26) Weber, L.; Frebel, M.; Boese, R. Übergangsmetall-substituierte Diphosphene. 25. Spaltung Der P=P-Bindung Eines Diphosphens Mit N-Methylmaleinsäureimid. Synthese Und Struktur Eines Bicyclo[3.1.0]-1-aza-4-phosphahexa-2,6-dions. *Zeitschrift fur Anorg. und Allg. Chemie* **1992**, *607* (1), 139–145. https://doi.org/10.1002/zaac.19926070124.

(27) Weber, L.; Rühlicke, A.; Stammler, H. G.; Neumann, B. Transition-Metal-Substituted Acylphosphanes and Phosphaalkenes. 18. P-Metalated Iminophosphiranes by Isocyanide Addition to a Metallophosphaalkene. X-Ray Structure Determination of [(H5-C5Me5)(CO)2FePC(SiMe3)2C=NPh. *Organometallics* **1993**, *12* (11), 4653–4656. https://doi.org/10.1021/om00035a059.

(28) Weber, L.; Buchwald, S.; Lentz, D.; Stamm, O.; Preugschat, D.; Marschall, R. Transition Metal-Substituted Diphosphenes. 35. On the Reactivity of Metallodiphosphenes (H5-C5Me5)(CO)2FeP=PR (R = C(SiMe3)3, 2,4,6-t-Bu3C6H2) toward Isocyanides. Formation and Structures of Iminodiphosphiranes and 2,4-Diimino-1,3-Diphosphetanes. *Organometallics* **1994**, *13* (11), 4406–4412.

(29) Nakazawa, H.; Buhro, W. E.; Bertrand, G.; Gladysz, J. A. Reactions of Phosphorus Electrophiles with [H5-C5Me5)Fe(CO)2]-: Spectroscopic Evidence for a Phosphinidene Complex. *Inorg. Chem.* **1984**, *23* (22), 3431–3433.

(30) Sterenberg, B. T.; Udachin, K. A.; Carty, A. J. Terminal Aminophosphinidene Complexes of Iron, Ruthenium, and Osmium. *Organometallics* **2003**, *22* (19), 3927–3932. https://doi.org/10.1021/om030386x.

(31) Niecke, E.; Hein, J.; Nieger, M. Reactions of Chloro({Tri-2,4,6-Tert-Butylphenyl}Imino)Phosphane with Anionic Transition-Metal Complexes: Stable Metalloiminophosphanes and Evidence for Terminal Aminophosphinidene Complexes. *Organometallics* **1989**, *8*, 2290–2291.

(32) Weber, L.; Reizig, K.; Bungardt, D.; Boese, R. Transition-Metal-Substituted Diphosphenes. 3. Synthesis of Stable Diphosphenes with Iron and Ruthenium Substituents. X-Ray Structure Analysis of (H5-C5Me5)(CO)2FeP=PC6H2-t-Bu3-2,4,6. *Organometallics* **1987**, *6* (1), 110–114.

(33) Weber, L.; Kirchhoff, R.; Boese, R.; Stammler, H. G.; Neumann, B. Transition Metal Substituted Diphosphenes. 31. Preparation of the (H1-1,2-Diphosphaallyl)Iron Complex (H5-C5Me5)(CO)2FeP(SiMe3)P=C(SiMe3)2 and Reaction with (Z-Cyclooctene)Cr(CO)5. Formation and Structures of the First H3-Ferradiphosphaallyl and H5-1,2-Di. *Organometallics* **1993**, *12* (3), 731–737. https://doi.org/10.1021/om00027a024.

(34) Weber, L.; Reizig, K.; Boese, R.; Polk, M. Z-[(H5-C5H5)(CO)2Fe-P=C(OSiMe3)(TBu)], a Phosphaalkenyl-Complex with a Fe–P Single Bond. *Angew. Chemie Int. Ed. English* **1985**, *24* (7), 604–605. https://doi.org/10.1002/anie.198506041.

(35) Weber, L.; Kleinebekel, S.; Rühlicke, A.; Stammler, H.-G.; Neumann, B. Syntheses and Structures of C-Monoamino-P-Ferriophosphaalkenes [(H5-C5Me5)(CO)2FeP=CR1(NR22)] (R1 = Ph, TBu, 3,4,5-(MeO)3C6H2; NR22 = NMe2, Piperidino). *Eur. J. Inorg. Chem* **2000**, 1185–1191. https://doi.org/10.1002/(SICI)1099-0682(200006)2000.

(36) Wilson, D. W. N.; Goicoechea, J. M. Synthesis of Metallophosphaalkenes by Reaction of Organometallic Nucleophiles with a Phosphaethynolato-Borane. *Chem. Commun.* **2019**, *55* (48), 6842–6845. https://doi.org/10.1039/c9cc03040a.

(37) Niecke, E.; Metternich, H. -J; Nieger, M.; Gudat, D.; Wenderoth, P.; Malisch, W.; Hahner, C.; Reich, W. Methylenphosphanyl-Komplexe von Chrom, Molybdän, Wolfram, Eisen Und Nickel: Synthese Und Reaktionen. *Chem. Ber.* **1993**, *126* (6), 1299–1309. https://doi.org/10.1002/cber.19931260606.

(38) Schilling, B. E. R.; Hoffmann, R.; Lichtenberger, D. L. CpM(CO)2(Ligand) Complexes. *J. Am. Chem. Soc.* **1979**, *101* (3), 585–591.

(39) Hutchins, L. D.; Paine, R. T.; Campana, C. F. Structure and Bonding in a Phosphenium Ion-Metal Complex, CH3NCH2CH2N(CH3)PMo(H5-C5H5)(CO)2. An Example of a Molybdenum-Phosphorus Multiple Bond. *J. Am. Chem. Soc.* **1980**, *102* (13), 4521–4523.

(40) Dubois, D. A.; Duesler, E. N.; Paine, R. T. Synthesis and Structure of a Bimetallic Diphosphenium Ion Complex Containing a Diazadiphosphetidine Ring. *Organometallics* **1983**, *2*, 1903–1905.

(41) Leise, M.; Lang, H.; Imhof, W.; Zsolnai, L. Metallinduzierte Und Basenkatalysierte 2-Propinyl-Allenyl-Umlagerung in [(HC≡CCH2)(2,4,6-TBu3C6H2O)]P=MoCp(CO)2. *Chem. Berichte* **1993**, *126* (5), 1077–1080.

(42) Leise, M.; Zsolnai, L.; Lang, H. Stepwise Synthesis and Reactivity of a Chlorine-Functionalized Σ3,Λ4-Phosphanediyl Complex; X-Ray Crystal Structure of (2,4,6-TBu3C6H2O)(Cl)P–MoCp(CO)3. *Polyhedron* **1993**, *12* (10), 1257–1260.

(43) Reisacher, H. U.; McNamara, W. F.; Duesler, E. N.; Paine, R. T. Reactions of Molybdenum and Tungsten Phosphenium Complexes with Sulfur and Selenium. *Organometallics* **1997**, *16* (3), 449–455. https://doi.org/10.1021/om9605490.

(44) Alonso, M.; García, M. E.; Ruiz, M. A.; Hamidov, H.; Jeffery, J. C. Chemistry of the Phosphinidene Oxide Ligand. *J. Am. Chem. Soc.* **2004**, *126* (42), 13610–13611. https://doi.org/10.1021/ja045487g.

(45) Alonso, M.; Alvarez, M. A.; García, M. E.; García-Vivó, D.; Ruiz, M. A. Chemistry of the Oxophosphinidene Ligand. 1. Electronic Structure of the Anionic Complexes [MCp{P(O)R*}(CO)2]- (M = Mo, W; R* = 2,4,6-C6H2tBu3) and Their Reactions with H+ and C-Based Electrophiles. *Inorg. Chem.* **2010**, *49* (19), 8962–8976. https://doi.org/10.1021/ic101261f.

(46) Alvarez, M. A.; García, M. E.; García-Vivó, D.; Ruiz, M. A.; Vega, P. Efficient Synthesis and Multisite Reactivity of a Phosphinidene-Bridged Mo-Re Complex. A Platform Combining Nucleophilic and Electrophilic Features. *Inorg. Chem.* **2020**, *59* (14), 9481–9485. https://doi.org/10.1021/acs.inorgchem.0c01554.

(47) Hutchins, L. D.; Duesler, E. N.; Paine, R. T. Synthesis and

Characterization of Metallophosphenium Ion Complexes Derived from Aminohalophosphites. Crystal and Molecular Structure of Mo(H5-C5H5)(CO)2[POCH2CH2NC(CH3)3]. *Organometallics* **1984**, *3* (3), 399–403. https://doi.org/10.1021/om00081a013.

(48) Gross, E.; Jörg, K.; Fiederling, K.; Göttlein, A.; Malisch, W.; Boese, R. Novel Synthesis of Complexes with Metal-Phosphorus Double Bonds. *Angew. Chemie Int. Ed. English* **1984**, *23* (9), 738–739.

(49) Karsch, H. H.; Reisacher, H. -U; Huber, B.; Müller, G.; Malisch, W.; Jörg, K. Phosphorus Analogues of Unsaturated Carbon Compounds: An (S-trans)-1,3-Diphospha-4-metallabutadiene and Its (S-cis)-Fe(CO)3 Complex. *Angew. Chemie Int. Ed. English* **1986**, *25* (5), 455–456. https://doi.org/10.1002/anie.198604551.

(50) Arif, A. M.; Cowley, A. H.; Quashie, S. Reactivity of a Phosphavinylidene. Reactions at Both Phosphorus-Carbon and Phosphorus-Molybdenum Double Bonds and a New Approach to Three-Electron Donor Phosphido Complexes. *J. Chem. Soc., Chem. Comm.* **1986**, 1437–1438.

(51) Hutchins, L. D.; Reisacher, H. U.; Wood, G. L.; Duesler, E. N.; Paine, R. T. Synthesis and Structure of Metallophosphenium Complexes Derived from Related Cyclic and Acyclic Aminohalophosphines. *J. Organomet. Chem.* **1987**, *335* (2), 229–237. https://doi.org/10.1016/0022-328X(87)87111-5.

(52) Cowley, A. H.; Giolando, D. M.; Nunn, C. M.; Pakulski, M.; Westmoreland, D.; Norman, N. C. Synthesis and Reactivity of Mononuclear Molybdenum Phosphido Complexes, [Mo(CO)2{P(Cl)R}(η-C5H5)] [R = CH(SiMe3)2 or NCMe2CH2CH2CH2CMe2]. *J. Chem. Soc. Dalt. Trans.* **1988**, 2127–2134. https://doi.org/10.1039/DT9880002127.

(53) Lang, H.; Leise, M.; Zsolnai, L. Bifunctional Neutral Phosphenium Ion Complexes: Synthesis of Phenylethynyl- and Styryl-Substituted (R)(R′)PMo- (H5-C5Me5)(CO)2 Compounds. Crystal Structure of [2,6-TBu2-4-MeC6H2O)(PhCC)]PMo(H5-C5Me5)(CO)2. *J. Organomet. Chem.* **1990**, *389* (3), 325–332. https://doi.org/10.1016/0022-328X(90)85427-Z.

(54) Lang, H.; Leise, M.; Zsolnai, L. 2-Propynyl Isomerization in [(R)(HC≡C-CH2)]P=MoCp(CO)2 : Synthesis of 1-Molybda-2-Phospha-1,3-Dienes. X-Ray Crystal Structure of (2,4,6-TBu3C6H2O)[(NEt2)(Me)C=CH]P=MoCp(CO)2. *Polyhedron* **1992**, *11* (10), 1281–1284.

(55) Gudat, D.; Niecke, E.; Malisch, W.; Hofmockel, U.; Quashie, S.; Cowley, A. H.; Arif, A. M.; Krebs, B.; Dartmann, M. Metallophospha-Alkenes: A Simple Access and Some Reactivities Involving the Phosphorus Atom. *J. Chem. Soc. Chem. Commun.* **1985**, 1687–1689.

(56) Arif, A. M.; Cowley, A. H.; Nunn, C. M.; Quashie, S.; Norman, N. C.; Orpen, A. G. Synthesis and Reactivity of a Phosphavinylidene Complex of Molybdenum. *Organometallics* **1989**, *8* (8), 1878–1884.

(57) Nifant'ev, I. E.; Manzhukova, L. F.; Antipin, M. Y.; Struchkov, Y. T.; Nifant'ev, E. E. Cyclopentadienylphosphonous Acid Amides in Organometallic Synthesis. *Metalloorg. Khim.* **1991**, *4*, 475–476.

(58) Nakazawa, H.; Yamaguchi, Y.; Kawamura, K.; Miyoshi, K. Comparison of the Reactivity of Cationic Phosphenium Complexes of Iron Containing a Group 14 Element Ligand. *Organometallics* **1997**, *16* (21), 4626–4635. https://doi.org/10.1021/om970480b.

(59) Lohrey, T. D.; Maron, L.; Bergman, R. G.; Arnold, J. Heterotetrametallic Re-Zn-Zn-Re Complex Generated by an Anionic Rhenium(I) β-Diketiminate. *J. Am. Chem. Soc.* **2019**, *2* (141), 800–804. https://doi.org/10.1021/jacs.8b12494.

(60) Boreen, M. A.; Lohrey, T. D.; Rao, G.; Britt, R. D.; Maron, L.; Arnold, J. A Uranium Tri-Rhenium Triple Inverse Sandwich Compound. *J. Am. Chem. Soc.* **2019**, *141* (13), 5144–5148. https://doi.org/10.1021/jacs.9b01331.

(61) Lohrey, T. D.; Rao, G.; Britt, R. D.; Bergman, R. G.; Arnold, J. H2 Activation and Direct Access to Terminal Nitride and Cyclo-P3 Complexes by an Acceptor-Free Rhenium(II) β-Diketiminate. *Inorg. Chem.* **2019**, *58* (19), 13492–13501. https://doi.org/10.1021/acs.inorgchem.9b02556.

(62) Lohrey, T. D.; Bergman, R. G.; Arnold, J. Controlling Dinitrogen Functionalization at Rhenium through Alkali Metal Ion Pairing. *Dalt. Trans.* **2019**, No. 48, 17936–17944. https://doi.org/10.1039/c9dt04489b.

(63) Lohrey, T. D.; Rao, G.; Small, D. W.; Ouellette, E. T.; Bergman, R. G.; Britt, R. D.; Arnold, J. Electronic Structures of Rhenium(II) β-Diketiminates Probed by EPR Spectroscopy: Direct Comparison of an Acceptor-Free Complex to Its Dinitrogen, Isocyanide, and Carbon Monoxide Adducts. *J. Am. Chem. Soc.* **2020**, *142* (32), 13805–13813. https://doi.org/10.1021/jacs.0c04719.

(64) Lohrey, T. D.; Fostvedt, J. I.; Bergman, R. G.; Arnold, J. Electron Acceptors Promote Proton-Hydride Tautomerism in Low Valent Rhenium β-Diketiminates. *Chem. Commun.* **2020**, *56* (26), 3761–3764. https://doi.org/10.1039/c9cc09475j.

(65) Ouellette, E. T.; Carpentier, A.; Joseph Brackbill, I.; Lohrey, T. D.; Douair, I.; Maron, L.; Bergman, R. G.; Arnold, J. σ or π? Bonding Interactions in a Series of Rhenium Metallotetrylenes. *Dalt. Trans.* **2021**, *50* (6), 2083–2092. https://doi.org/10.1039/d1dt00129a.

(66) Ouellette, E. T.; Amaro Estrada, J. I.; Lussier, D. J.; Chakarawet, K.; Lohrey, T. D.; Maron, L.; Bergman, R. G.; Arnold, J. Spectroscopic, Magnetic, and Computational Investigations on a Series of Rhenium(III) Cyclopentadienide β-Diketiminate Halide and Pseudohalide Complexes. *Organometallics* **2021**, 1–40. https://doi.org/10.1021/acs.organomet.1c00516.

(67) Ouellette, E. T.; Magdalenski, J. S.; Bergman, R. G.; Arnold, J. Heterobimetallic-Mediated Dinitrogen Functionalization: N-C Bond Formation at Rhenium-Group 9 Diazenido Complexes. *Inorg. Chem.* **2022**, *61* (40), 16064–16071. https://doi.org/10.1021/acs.inorgchem.2c02463.

(68) Ouellette, E. T.; Magdalenski, J. S.; Bergman, R. G.; Arnold, J. Applications of Low-Valent Transition Metalates: Development of a Reactive Noncarbonyl Rhenium(I) Anion. *Acc. Chem. Res.* **2022**, *55* (5), 783–793. https://doi.org/10.1021/acs.accounts.2c00013.

(69) Kaniewska-Laskowska, K.; Pikies, J.; Grubba, R. Iron Complexes with Terminal and Nonbridging Phosphanido Ligands. *Inorganica Chim. Acta* **2021**, *520*, 120266. https://doi.org/10.1016/j.ica.2021.120266.

(70) Mason, J. Chapter 13: Phosphorus to Bismuth. In *Multinuclear NMR*; 1987; pp 369–397.

(71) Light, R. W.; Paine, R. T. Interaction of the Dicoordinate Phosphorus Cation 1,3-Dimethyl-1,3,2-Diazaphospholidide with Transition Metal Nucleophiles. *J. Am. Chem. Soc.* **1978**, *100* (7), 2230–2231.

(72) Green, M. L. H. A New Approach to the Formal Classification of Covalent Compounds of the Elements. *J. Organomet. Chem.* **1995**, *500* (1–2), 127–148. https://doi.org/10.1016/0022-328X(95)00508-N.

(73) Pyykkö, P. Additive Covalent Radii for Single-, Double-, and Triple-Bonded Molecules and Tetrahedrally Bonded Crystals: A Summary. *J. Phys. Chem. A* **2015**, *119* (11), 2326–2337. https://doi.org/10.1021/jp5065819.

(74) Dean, W. K.; Heyl, B. L.; Vanderveer, D. G. Molecular Structure of Bis[μ-5,5-Dimethyl-1,3,2-Dioxaphosphorinano]-Hexacarbonyldiiron, [OCH2CMe2CH2OPFe(CO)3]2. *Inorg. Chem.* **1978**, *17* (7), 1909–1913.

(75) Liu, X.; Riera, V.; Ruiz, M. A.; Lanfranchi, M.; Tiripicchio, A.; Tiripicchio-camellini, M.; Generóle, C.; Cnr, D.; Parma, U.; Scienze, V. Redox-Induced P-P and Mn-Mn Bond Cleavages at Dimanganese Carbonyl Centers. Synthesis and Oxidation Reactions of the Dianion [Mn2{μ-P(OEt)2}{μ,H2-OP(OEt)2}(CO)6]2-. *Organometallics* **1994**, *13* (5), 1940–1949.

(76) Corrigan, J. F.; Dinardo, M.; Doherty, S.; Hogarth, G.; Sun, Y.; Taylor, N. J.; Carty, A. J. Electron Rich Cluster Chemistry: Synthesis and Molecular and Electronic Structures of the Series of Clusters Ru4(CO)13(μ-PR2)2 with Expanded Metal Frameworks. *Organometallics* **1994**, *13* (9), 3572–3580. https://doi.org/10.1021/om00021a033.

(77) Davies, J. E.; Feeder, N.; Gray, C. A.; Mays, M. J.; Woods, A. D.

The Reactions of the Anions [Cp2(CO)4Mo2(u-PRR')]- (R, R' = H, Ph) towards Chloroarsines and Chlorophosphines; Synthesis of Complexes Containing Both Bridging Phosphide and Arsenido Groups. *J. Chem. Soc. Dalt. Trans.* **2000**, *2* (11), 1695–1702. https://doi.org/10.1039/b001193m.

(78) Liu, X.-Y.; Riera, V.; Ruiz, M. A. Manganese-Group 11 Element and -Zinc Mixed-Metal Clusters Derived from the Binuclear Dianion [Mn2{μ-P(OEt)2}{μ-H2-OP(OEt)2}(CO)6]2-. X-Ray Structures of [Mn2Zn{μ-P(OEt)2}{μ-H2-OP(OEt)2}(CO)6(C10H8N2-N,N')] and [Mn2Au3{μ-P(OEt)2}(CO)6(PPh3)3]. *Organometallics* **1996**, *15* (3), 974–983. https://doi.org/10.1515/znb-1983-1213.

(79) Alvarez, C. M.; Garcia, M. E.; Riera, V.; Ruiz, M. A.; Bois, C. Unusual Reactivity of the Unsaturated Dimolybdenum Complex Mo2(H5-C5H5)2{μ-OP(OEt)2}{μ-P(OEt)2}(CO)2. *Organometallics* **2003**, *22* (13), 2741–2748.

(80) Pangan, L. N.; Kawano, Y.; Shimoi, M. Synthesis of Nido-[1-OMe-2,3-(Cp*Ru)2{μ-P(OMe)2} B3H5]: Methoxy Transfer from Phosphorus to Boron and Cluster Core Rearrangement. *Inorg. Chem.* **2001**, *40* (9), 1985–1986. https://doi.org/10.1021/ic001334s.

(81) Shi, Y. C.; Shi, Y.; Yang, W. Syntheses of New Fe/Se Clusters via the Reactions of PhC(Se)NHCH2Ph, Et3N and Fe3(CO)12 with Electrophiles. *J. Organomet. Chem.* **2014**, *772*, 131–138. https://doi.org/10.1016/j.jorganchem.2014.08.033.

(82) Mathur, P.; Ji, R. S.; Raghuvanshi, A.; Tauqeer, M.; Mobin, S. M. Cleavage of Phosphorus-Sulfur Bond and Formation of (M4-S)Fe4core from Photochemical Reactions of Fe(CO)5with [(RO)2PS2]2; (R = Me, Et,IPr). *J. Organomet. Chem.* **2017**, *835*, 31–38. https://doi.org/10.1016/j.jorganchem.2017.02.036.

(83) Song, L. C.; Gu, Z. C.; Zhang, W. W.; Li, Q. L.; Wang, Y. X.; Wang, H. F. Synthesis, Structure, and Electrocatalysis of Butterfly [Fe2SP] Cluster Complexes Relevant to [FeFe]-Hydrogenases. *Organometallics* **2015**, *34* (16), 4147–4157. https://doi.org/10.1021/acs.organomet.5b00560.

(84) Day, V. W.; Tavanaiepour, I.; Abdel-Meguid, S. S.; Kirner, J. F.; Goh, L.-Y.; Muetterties, E. L. Modes of Phosphite Reactions with Transition-Metal Complexes. Crystal Structures of (H5-C5H5)Cr[P(O)(OCH3)2](CO)2[P(OCH3)3] and {(CH3O)2PMo[P(OCH3)3]5+}(PF6–). *Inorg. Chem.*. **1982**, *21* (2), 657–663.

(85) Gilheany, D. G. No d Orbitals but Walsh Diagrams and Maybe Banana Bonds: Chemical Bonding in Phosphines, Phosphine Oxides, and Phosphonium Ylides. *Chem. Rev.* **2002**, *94* (5), 1339–1374. https://doi.org/10.1021/cr00029a008.

(86) Jorg, K.; Malisch, W.; Reich, W.; Meyer, A.; Schubert, U. Synthesis, Structure, and Addition Reactions of [Cp(CO)2W=PR2], R = IPr, TBu. *Angew. Chemie - Int. Ed.* **1986**, *25* (1), 92–93.

(87) Oliemuller, L. K.; Moore, C. E.; Thomas, C. M. Electronic and Structural Variations of a Nickel(0) N-Heterocyclic Phosphenium Complex in Comparison to Group 10 Analogues. *Inorg. Chem.* **2022**, *61* (48), 19440–19451. https://doi.org/10.1021/acs.inorgchem.2c03302.

(88) Gudat, D.; Niecke, E. Transfer of a Pentamethylcyclopentadienyl Ligand from Phosphorus to Nickel: Generation and Spectroscopic Characterization of the First Examples of Metalloiminophosphanes [(H5-Me5C5)(R3P)Ni-P=NBut] (R = Et, Bu, or Ph). *J. Chem. Soc., Chem. Comm.* **1987**, *4*, 10–11.

(89) Abbenseth, J.; Diefenbach, M.; Hinz, A.; Alig, L.; Würtele, C.; Goicoechea, J. M.; Holthausen, M. C.; Schneider, S. Oxidative Coupling of Terminal Rhenium Pnictide Complexes. *Angew. Chemie - Int. Ed.* **2019**, *58* (32), 10966–10970. https://doi.org/10.1002/anie.201905130.

(90) Niecke, B. E.; Nieger, M.; Reichert, F. Arylimino(Halogeno)Phosphanes XP=NC6H2tBu3 (X = C1, Br, I) and the Iminophosphenium Tetrachloroaluminate [P≡NC6H2tBu3]+[AlCl4]- : The First Stable Compound with a PN Triple Bond. *Angew. Chemie Int. Ed. English* **1988**, *27* (12), 1715–1716.

(91) Martinez, J. L.; Lutz, S. A.; Beagan, D. M.; Gao, X.; Pink, M.; Chen, C. H.; Carta, V.; Moënne-Loccoz, P.; Smith, J. M. Stabilization of the Dinitrogen Analogue, Phosphorus Nitride. *ACS Cent. Sci.* **2020**, *6* (9), 1572–1577. https://doi.org/10.1021/acscentsci.0c00944.

(92) Nrar, M. P.; Laplaza, C. E.; Davis, W. M.; Cummins, C. C. A Molybdenum - Phosphorus Triple Bond : Synthesis, Structure, and Reactivity. *Angew. Chemie - Int. Ed.* **1995**, *34* (18), 2042–2044.

(93) Saint-Denis, T. G.; Wheeler, T. A.; Chen, Q.; Balázs, G.; Settineri, N. S.; Scheer, M.; Tilley, T. D. A Ruthenophosphanorcaradiene as a Synthon for an Ambiphilic Metallophosphinidene. *J. Am. Chem. Soc.* **2024**, *146*, 4369–4374. https://doi.org/10.1021/jacs.3c14779.

(94) Gudat, D.; Niecke, E. Reaction of (Pentamethylocyclopentadienyl)(Tert-Butylimino)-Phosphane with Tris(Acetonitrile)Tricarbonylmolybdenum(0): Evidence for a Metalloiminophosphane Intermediate. *Organometallics* **1986**, *5* (11), 2376–2377.

(95) Enemark, J. H.; Feltham, R. D. Principles of Structure, Bonding, and Reactivity for Metal Nitrosyl Complexes. *Coord. Chem. Rev.* **1974**, *13* (4), 339–406. https://doi.org/10.1016/S0010-8545(00)80259-3.

(96) Malisch, W.; Hirth, U. A.; Grün, K.; Schmeußer, M. Phosphenium Complexes 30. Supermesitylphosphenium Complexes of Molybdenum and Tungsten: Synthesis and Exchange Reactions Involving the P-H Bond. *J. Organomet. Chem.* **1999**, *572* (2), 207–212. https://doi.org/10.1016/S0022-328X(98)00947-4.

(97) Transue, W. J.; Dai, Y.; Riu, M. L. Y.; Wu, G.; Cummins, C. C. 31P NMR Chemical Shift Tensors: Windows into Ruthenium Phosphinidene Complex Electronic Structures. *Inorg. Chem.* **2021**, *60* (13), 9254–9258. https://doi.org/10.1021/acs.inorgchem.1c01099.

(98) Sterenberg, B. T.; Udachin, K. A.; Carty, A. J. Electrophilic "Fischer Type" Phosphinidene Complexes of Molybdenum, Tungsten, and Ruthenium. *Organometallics* **2001**, *20* (13), 2657–2659. https://doi.org/10.1021/om010225y.

(99) Sterenberg, B. T.; Carty, A. J. Terminal Chloroaminophosphido and Aminophosphinidene Complexes of Molybdenum. *J. Organomet. Chem.* **2001**, *617–618*, 696–701. https://doi.org/10.1016/S0022-328X(00)00709-9.

(100) Sánchez-Nieves, J.; Sterenberg, B. T.; Udachin, K. A.; Carty, A. J. A Thermally Stable and Sterically Unprotected Terminal Electrophilic Phosphinidene Complex of Cobalt and Its Conversion to an H1-Phosphirene. *J. Am. Chem. Soc.* **2003**, *125* (9), 2404–2405. https://doi.org/10.1021/ja028303b.

(101) Graham, T. W.; Udachin, K. A.; Zgierski, M. Z.; Carty, A. J. Synthesis and Structural Characterization of the First Thermally Stable, Neutral, and Electrophilic Phosphinidene Complexes of Vanadium. *Organometallics* **2011**, *30* (6), 1382–1388. https://doi.org/10.1021/om100915v.

(102) Braunschweig, H.; Jimenez-Halla, J. O. C.; Radacki, K.; Shang, R. Direct Conversion from Terminal Borylene into Terminal Phosphinidene. *Angew. Chemie - Int. Ed.* **2016**, *55* (41), 12673–12677. https://doi.org/10.1002/anie.201603548.

(103) Graham, T. W.; Cariou, R. P. Y.; Sánchez-Nieves, J.; Allen, A. E.; Udachin, K. A.; Regragui, R.; Carty, A. J. Reactivity of Terminal Electrophilic Phosphinidene Complexes: Synthesis of the First Rhenium Phosphinidene, [Re(CO)5(H1-PN IPr2)][AlCl4], and Novel Reactions with Azobenzene. *Organometallics* **2005**, *24* (9), 2023–2026. https://doi.org/10.1021/om0401307.

(104) Sterenberg, B. T.; Senturk, O. S.; Udachin, K. A.; Carty, A. J. Reactivity of Terminal, Electrophilic Phosphinidene Complexes of Molybdenum and Tungsten. Nucleophilic Addition at Phosphorus and P-P Bond Forming Reactions with Phosphines and Diphosphines. *Organometallics* **2007**, *26* (4), 925–937. https://doi.org/10.1021/om060685x.

(105) Creve, S.; Pierloot, K.; Nguyen, M. T.; Vanquickenborne, L. G. Phosphinidene Transition Metal Complexes: A Combined Ab Initio MO-DFT Study of Cr(CO)5-PR. *Eur. J. Inorg. Chem.* **1999**, 107–115. https://doi.org/10.1002/(SICI)1099-0682(199901)1999:1<107::AID-EJIC107>3.0.CO;2-4.

(106) Ehlers, A. W.; Baerends, E. J.; Lammertsma, K. Nucleophilic or Electrophilic Phosphinidene Complexes MLn=PH; What Makes the Difference? *J. Am. Chem. Soc.* **2002**, *124* (11), 2831–2838. https://doi.org/10.1021/ja017445n.

(107) Pandey, K. K.; Tiwari, P.; Patidar, P. Structure and Bonding Analysis of the Cationic Electrophilic Phosphinidene Complexes of Iron, Ruthenium, and Osmium [(H5-C 5Me5)(CO)2M{PNiPr2}] +, [(H5-C5H5)(CO) 2M{PNR2}]+ (R = Me, IPr).. *J. Phys. Chem. A* **2012**, *116* (47), 11753–11762. https://doi.org/10.1021/jp309092t.

(108) Pandey, K. K.; Tiwari, P.; Patidar, P.; Patidar, S. K.; Vishwakarma, R.; Bariya, P. K. Accurate Theoretical Description of the M-PNR2 Bonds in Phosphinidene Complexes of Manganese and Rhenium [(CO)5M-PNR2]+ (R = Me, IPr, TBu) and [(PMe3)(CO)4M-PNiPr2]+: A DFT-D3 Study. *J. Organomet. Chem.* **2014**, *751*, 781–787. https://doi.org/10.1016/j.jorganchem.2013.07.029.

(109) Rajagopalan, R. A.; Jayaraman, A.; Sterenberg, B. T. Reactivity of a Dichlorophosphido Complex. Nucleophilic Substitution Reactions at Metal Coordinated Phosphorus. *J. Organomet. Chem.* **2014**, *761*, 84–92. https://doi.org/10.1016/j.jorganchem.2014.02.025.

(110) Ho, J.; Drake, R. J.; Stephan, D. W. [Cp2Zr(μ-PPh)]2[((THF)3Li)2(μ-N2)]: A Remarkable Salt of a Zirconocene Phosphinidene Dianion and Lithium Dication Containing Side-Bound Dinitrogen. *J. Am. Chem. Soc* **1993**, *115* (9), 3792–3793.

(111) Ho, J.; Hou, Z.; Drake, R. J.; Stephan, D. W. P-H and Cyclopentadienyl C-H Activation En Route to Homo- and Heterobinuclear Zirconocene Phosphide and Phosphinidene Complexes. *Organometallics* **1993**, *12* (8), 3145–3157. https://doi.org/10.1021/om00032a043.

(112) Sekar, P.; Scheer, M.; Voigt, A.; Kirmse, R. Unusual Reactivity of a Cr2P2 Tetrahedral Complex toward Superhydride; Formation of [{CpCr(CO)2}2(μ-PH2) x(μ-H)2-x] (x = 1 and 2) and [〈 {CpCr(CO)2}2(μ-PH) 〉 {(CpCr) 2(μ,H1:H1:η 5:H5:P5)}]. *Organometallics* **1999**, *18* (15), 2833–2837. https://doi.org/10.1021/om990098u.

(113) Bai, G.; Wei, P.; Das, A. K.; Stephan, D. W. P-H and P-P Bond Activation by Ni(I) and Fe(I) β-Diketiminato- Complexes. *Dalt. Trans.* **2006**, *6* (9), 1141–1146. https://doi.org/10.1039/b513892b.

(114) Cui, P.; Chen, Y.; Xu, X.; Sun, J. An Unprecedented Lanthanide Phosphinidene Halide: Synthesis, Structure and Reactivity. *Chem. Commun.* **2008**, 5547–5549. https://doi.org/10.1039/b813075b.

(115) Cui, P.; Chen, Y.; Borzov, M. V. Neodymium(III) Phosphinidene Complexes Supported by Pentamethylcyclopentadienyl and Hydrotris(Pyrazolyl)Borate Ligands. *Dalt. Trans.* **2010**, *39* (29), 6586–6590. https://doi.org/10.1039/c003089a.

(116) Basuli, F.; Bailey, B. C.; Huffman, J. C.; Baik, M. H.; Mindiola, D. J. Terminal and Four-Coordinate Vanadium(IV) Phosphinidene Complexes. A Pseudo Jahn-Teller Effect of Second Order Stabilizing the V-P Multiple Bond. *J. Am. Chem. Soc.* **2004**, *126* (7), 1924–1925. https://doi.org/10.1021/ja0392216.

(117) Chatt, J.; Leigh, G. J.; Mingos, D. M. P.; Paske, R. J. Complexes of Osmium, Ruthenium, Rhenium, and Iridium Halides with Some Tertiary Monophosphines and Monoarsines. *J. Chem. Soc. A Inorganic, Phys. Theor.* **1968**, 2636–2641. https://doi.org/10.1039/J19680002636.

(118) Pieper, H. H.; Schwochau, K. Hyperfine and Superhyperfine EPR Spectra of Tc(IV) and Re(IV) in Tin Dioxide Single Crystals. *J. Chem. Phys.* **1975**, *63* (11), 4716–4722. https://doi.org/10.1063/1.431257.

(119) Bufaical, F. R.; Harris, E. A. ELECTRON PARAMAGNETIC RESONANCE OF Re 4+ : (NH4) 2 PtCl 6. *Solid State Commun.* **1981**, *39*, 1143–1146.

(120) Kochel, A.; Lis, T.; Mrozin, J. Synthesis , Structure and Magnetic Properties of Trans-Tetrachloro-Bis-(Pyridine)-Rhenium (IV). *J. Mol. Struct.* **2002**, *610*, 53–58.

(121) Martínez-Lillo, J.; Mastropietro, T. F.; Lhotel, E.; Paulsen, C.; Cano, J.; Munno, G. De; Faus, J.; Lloret, F.; Julve, M.; Nellutla, S.; Krzystek, J. Highly Anisotropic Rhenium(IV) Complexes: New Examples of Mononuclear Single-Molecule Magnets. *J. Am. Chem. Soc* **2013**, *135*, 13737–13748. https://doi.org/dx.doi.org/10.1021/ja403154z.

(122) Pedersen, K. S.; Sigrist, M.; Sørensen, M. A.; Barra, A. L.; Weyhermuller, T.; Piligkos, S.; Thuesen, C. A.; Vinum, M. G.; Mutka, H.; Weihe, H.; Clerac, R.; Bendix, J. [ReF6]2-: A Robust Module for the Design of Molecule-Based Magnetic Materials. *Angew. Chemie - Int. Ed.* **2014**, *53* (5), 1351–1354. https://doi.org/10.1002/anie.201309981.

(123) Singh, S. K.; Rajaraman, G. Deciphering the Origin of Giant Magnetic Anisotropy and Fast Quantum Tunnelling in Rhenium(IV) Single-Molecule Magnets. *Nat. Commun.* **2016**, *7*, 1–8. https://doi.org/10.1038/ncomms10669.

(124) Savage, P. D.; Wilkinson, G.; Motevalli, M.; Hursthouse, M. B. Synthesis of Homoleptic Tetrahedral Aryls of Rhenium(IV) and Ruthenium(IV). X-Ray Crystal Structures of Tetrakis(o-Methylphenyl)Rhenium(IV), Tetrakis(o-Methyl Phenyl)Oxorhenium (VI), and Tetrakis(o-Methylphenyl)-Ruthenium(IV). *J. Chem. Soc., Dalt. Trans.* **1988**, 669–672.

(125) Alig, L.; Eisenlohr, K. A.; Zelenkova, Y.; Rosendahl, S.; Herbst-Irmer, R.; Demeshko, S.; Holthausen, M. C.; Schneider, S. Rhenium-Mediated Conversion of Dinitrogen and Nitric Oxide to Nitrous Oxide. *Angew. Chemie - Int. Ed.* **2022**, *61* (2), 1–5. https://doi.org/10.1002/anie.202113340.

(126) Ding, M.; Cutsail, G. E.; Aravena, D.; Amoza, M.; Rouzières, M.; Dechambenoit, P.; Losovyj, Y.; Pink, M.; Ruiz, E.; Clérac, R.; Smith, J. M. A Low Spin Manganese(IV) Nitride Single Molecule Magnet. *Chem. Sci.* **2016**, *7* (9), 6132–6140. https://doi.org/10.1039/c6sc01469k.

(127) Park, S.; Jin, K.; Lim, H. K.; Kim, J.; Cho, K. H.; Choi, S.; Seo, H.; Lee, M. Y.; Lee, Y. H.; Yoon, S.; Kim, M.; Kim, H.; Kim, S. H.; Nam, K. T. Spectroscopic Capture of a Low-Spin Mn(IV)-Oxo Species in Ni–Mn3O4 Nanoparticles during Water Oxidation Catalysis. *Nat. Commun.* **2020**, *11* (1), 1–10. https://doi.org/10.1038/s41467-020-19133-w.

(128) Scepaniak, J. J.; Vogel, C. S.; Khusniyarov, M. M.; Heinemann, F. W.; Meyer, K.; Smith, J. M. Synthesis, Structure, and Reactivity of an Iron(V) Nitride. *Science* **2011**, *331* (6020), 1049–1052.

(129) Van Heuvelen, K. M.; Fiedler, A. T.; Shan, X.; De Hont, R. F.; Meier, K. K.; Bominaar, E. L.; Muñck, E.; Que, L. One-Electron Oxidation of an Oxoiron(IV) Complex to Form an [O=Fe V=NR]+ Center. *Proc. Natl. Acad. Sci.* **2012**, *109* (30), 11933–11938. https://doi.org/10.1073/pnas.1206457109.

(130) Cutsail, G. E.; Stein, B. W.; Subedi, D.; Smith, J. M.; Kirk, M. L.; Hoffman, B. M. EPR, ENDOR, and Electronic Structure Studies of the Jahn-Teller Distortion in an FeV Nitride. *J. Am. Chem. Soc.* **2014**, *136* (35), 12323–12336. https://doi.org/10.1021/ja505403j.

(131) Chang, H. C.; Mondal, B.; Fang, H.; Neese, F.; Bill, E.; Ye, S. Electron Paramagnetic Resonance Signature of Tetragonal Low Spin Iron(V)-Nitrido and-Oxo Complexes Derived from the Electronic Structure Analysis of Heme and Non-Heme Archetypes. *J. Am. Chem. Soc.* **2019**, *141* (6), 2421–2434. https://doi.org/10.1021/jacs.8b11429.

(132) Kim, Y.; Kim, J.; Nguyen, L. K.; Lee, Y. M.; Nam, W.; Kim, S. H. EPR Spectroscopy Elucidates the Electronic Structure of [FeV(O)(TAML)] Complexes. *Inorg. Chem. Front.* **2021**, *8* (15), 3775–3783. https://doi.org/10.1039/d1qi00522g.

(133) Peters, J. C.; Odom, A. L.; Cummins, C. C. A Terminal Molybdenum Carbide Prepared by Methylidyne Deprotonation. *Chem. Commun.* **1997**, No. 20, 1995–1996. https://doi.org/https://doi.org/10.1039/A704251E.

(134) McNaughton, R. L.; Chin, J. M.; Weare, W. W.; Schrock, R. R.; Hoffman, B. M. EPR Study of the Low-Spin [D3; S =1/2], Jahn-Teller-Active, Dinitrogen Complex of a Molybdenum Trisamidoamine. *J. Am. Chem. Soc.* **2007**, *129* (12), 3480–3481. https://doi.org/10.1021/ja068546u.

(135) Kuiper, D. S.; Wolczanski, P. T.; Lobkovsky, E. B.; Cundari, T. R. Low Coordinate, Monomeric Molybdenum and Tungsten(III) Complexes: Structure, Reactivity and Calculational Studies of (Silox)3Mo and (Silox)3ML (M = Mo, W; L = PMe3, CO; Silox = TBu3SiO). *J. Am. Chem. Soc.* **2008**,

130 (39), 12931–12943. https://doi.org/10.1021/ja802706u.
(136) McNaughton, R. L.; Roemelt, M.; Chin, J. M.; Schrock, R. R.; Neese, F.; Hoffman, B. M. Experimental and Theoretical EPR Study of Jahn-Teller-Active [HIPTN3N]MoL Complexes (L = N2, CO, NH3). *J. Am. Chem. Soc.* **2010**, *132* (25), 8645–8656. https://doi.org/10.1021/ja1004619.
(137) Morton, J. R.; Preston, K. F. Atomic Parameters for Paramagnetic Resonance Data. *J. Magn. Reson.* **1978**, *30* (3), 577–582. https://doi.org/10.1016/0022-2364(78)90284-6.

For Table of Contents Only:

Synopsis: M–PR_n (n=1,2) complexes are useful reagents for the synthesis of organophosphorus compounds. Even so, few metal fragments exist for which several M–PR_n have been synthesized, such that the influence of the phosphorus substituent might be systematically unraveled. This study reports the synthesis, characterization, and computation investigation of several Re–PR_n complexes derived from a L_2MCp-type fragment.

Insert Table of Contents artwork here